Received: 11 July 2019 | Revised: 28 October 2019 | Accepted: 4 November 2019

DOI: 10.1111/cmi.13146

RESEARCH ARTICLE

WILEY

A patatin-like phospholipase functions during gametocyte induction in the malaria parasite *Plasmodium falciparum*

Ansgar Flammersfeld[1] | Atscharah Panyot[1] | Yoshiki Yamaryo-Botté[2] | Philipp Aurass[4] | Jude M. Przyborski[3] | Antje Flieger[4] | Cyrille Botté[2] | Gabriele Pradel[1]

[1]Division of Cellular and Applied Infection Biology, Institute of Zoology, RWTH Aachen University, Aachen, Germany

[2]ApicoLipid Team, Institute for Advanced Biosciences, Université Grenoble Alpes, La Tronche, France

[3]Division of Enteropathogenic Bacteria and Legionella, Robert Koch-Institute, Wernigerode, Germany

[4]Centre for Infectious Diseases, Heidelberg University Hospital, Heidelberg, Germany

Correspondence
Gabriele Pradel, Division of Cellular and Applied Infection Biology, Institute of Zoology, RWTH Aachen University, Worringerweg 1, 52074 Aachen, Germany.
Email: pradel@bio2.rwth-aachen.de

Funding information
Deutsche Forschungsgemeinschaft, Grant/Award Number: SPP1580

Abstract

Patatin-like phospholipases (PNPLAs) are highly conserved enzymes of prokaryotic and eukaryotic organisms with major roles in lipid homeostasis. The genome of the malaria parasite *Plasmodium falciparum* encodes four putative PNPLAs with predicted functions during phospholipid degradation. We here investigated the role of one of the plasmodial PNPLAs, a putative PLA_2 termed PNPLA1, during blood stage replication and gametocyte development. PNPLA1 is present in the asexual and sexual blood stages and here localizes to the cytoplasm. PNPLA1-deficiency due to gene disruption or conditional gene-knockdown had no effect on intraerythrocytic growth, gametocyte development and gametogenesis. However, parasites lacking PNPLA1 were impaired in gametocyte induction, while PNPLA1 overexpression promotes gametocyte formation. The loss of PNPLA1 further leads to transcriptional down-regulation of genes related to gametocytogenesis, including the gene encoding the sexual commitment regulator AP2-G. Additionally, lipidomics of PNPLA1-deficient asexual blood stage parasites revealed overall increased levels of major phospholipids, including phosphatidylcholine (PC), which is a substrate of PLA_2. PC synthesis is known to be pivotal for erythrocytic replication, while the reduced availability of PC precursors drives the parasite into gametocytogenesis; we thus hypothesize that the higher PC levels due to PNPLA1-deficiency prevent the blood stage parasites from entering the sexual pathway.

KEYWORDS

malaria, *Plasmodium falciparum*, gametocyte induction, patatin-like phospholipase, sexual commitment, phosphatidylcholine

1 | INTRODUCTION

Following a first round of multiplication in the human liver, the unicellular malaria parasite *Plasmodium falciparum* enters the blood stream and replicates in human red blood cells (RBCs). The repetitive 48-hr infection cycles, which result in the destruction of the RBC during the release of the newly formed parasites, are responsible for the typical symptoms of malaria such as fever, anaemia and organ failure (reviewed in Cowman, Healer, Marapana, & Marsh, 2016; Haldar & Mohandas, 2009). Infections with *P. falciparum* are the main cause of

the ~435,000 deaths due to malaria per year, 90% of which occur in the African region (World Health Organisation, 2018).

During its intraerythrocytic development, *Plasmodium* induces substantial changes in the structural and functional properties of the RBC. Intraerythrocytic growth leads to an intense period of membrane biogenesis, which includes the formation of external vacuolar transport systems and cell-internal membranous compartments. Membrane synthesis is further crucial for the development of the roughly 16 daughter cells that are formed during erythrocytic schizogony, and these membrane dynamics require synthesis, modification and degradation of phospholipids. While the parasite is capable to *de novo* synthesize the majority of phospholipids, their precursors like the polar heads choline and ethanolamine as well as the fatty acids need to be scavenged from the host blood serum (reviewed in e.g. Ben Mamoun, Prigge, & Vial, 2010; Déchamps et al., 2010; Flammersfeld, Lang, Flieger, & Pradel, 2018; Vial, Eldin, Tielens, & Van Hellemond, 2003). The total amount of phospholipids increases approximately fivefold in the infected RBCs with phosphatidylcholine (PC) and phosphatidylethanolamine (PE) being the main membrane components (Beaumelle & Vial, 1988; Botté et al., 2013; Gulati et al., 2015; Simões, Roelofsen, & Op den Kamp, 1992; reviewed in Déchamps, Maynadier, et al., 2010).

During the erythrocytic infection cycle, a proportion of blood stage parasites enter the sexual pathway, which results in the production of the transmissible gametocytes. Gametocyte induction is upregulated in response to stress factors and particularly depends on the availability of PC precursors in the human serum, that is, low levels of serum-derived lysoPC and choline cause the blood stage parasites to enter the sexual pathway (Brancucci et al., 2017; Wein et al., 2018). These gametocytes, once matured, transform into gametes following their uptake by blood-feeding *Anopheles* mosquitoes. Gametogenesis is followed by sexual reproduction of the parasite, an event preluding the mosquito-specific phase of the plasmodial life-cycle (reviewed in Bennink, Kiesow, & Pradel, 2016; Kuehn & Pradel, 2010).

Membrane biogenesis in the intraerythrocytic blood stages requires the action of phospholipases, lipolytic enzymes that are classified into four groups, A, B, C and D corresponding to the hydrolysis activity (reviewed in Déchamps, Shastri, Wengelnik, & Vial, 2010; Flammersfeld et al., 2018; Vial & Ben Mamoun, 2005). A recent analysis of the *P. falciparum* genome identified 22 putative phospholipases. The main proportion of these enzymes exhibit a predicted α/β hydrolase domain and 12 of these were annotated as lysophospholipases (Flammersfeld et al., 2018). In addition, four putative patatin-like phospholipases (PNPLAs) are encoded in the *P. falciparum* genome. PNPLAs can typically be found both in eukaryotes and in a variety of bacteria, where they have major roles in lipid homeostasis, but where they can also be involved in membrane degradation and cell signalling (reviewed in Banerji & Flieger, 2004; Kienesberger, Oberer, Lass, & Zechner, 2009). They share conserved common protein domains with patatin, a storage glycoprotein of potato tuber with lipid acyl hydrolase activity (Senda, Yoshioka, Doke, & Kawakita, 1996; reviewed in Shewry, 2003). All PNPLAs exhibit a catalytic Ser-Asp dyad with the serine residue being embedded within the conserved penta-peptide Gly-Xaa-Ser-Xaa-Gly (GXSXG; reviewed in Arpigny & Jaeger, 1999; Banerji & Flieger, 2004; Ramanadham et al., 2015). Via their phospholipase A_2 (PLA_2) activity, PNPLAs are able to generate lysophospholipids and fatty acids, including polyunsaturated fatty acids, which are either further processed within the lipid metabolism pathway or which may act as signalling molecules (Lévêque et al., 2017; reviewed in Kienesberger et al., 2009; Ramanadham et al., 2015; Wilson & Knoll, 2018).

We here report on the functional characterisation of one of the four plasmodial PNPLAs, termed PNPLA1 (PlasmoDB gene-ID: PF3D7_0209100; plasmodb.org; Aurrecoechea et al., 2009). The protein is found in the cytosol of the asexual and sexual blood stages of *P. falciparum*. Asexual blood stages lacking PNPLA1 exhibit upregulated phospholipid levels as well as impaired gametocyte induction both under normal growth conditions and following growth in phospholipid precursor-deficient medium, suggesting that the deregulated phospholipid levels in the asexual blood stages render these less sensitive to modulators of gametocytogenesis.

2 | RESULTS

2.1 | PNPLA1 is a patatin-like phospholipase of the *P. falciparum* blood stages

The gene PF3D7_0209100 of *P. falciparum* encodes a putative patatin-like phospholipase, henceforth termed PNPLA1, with a molecular weight of 78 kDa. PNPLA1 is predicted to be a PLA_2 with a patatin-like phospholipase domain spanning from aa 338 to aa 544 and a C-terminal FabD/lysophospholipase-like domain ranging from aa 332 to aa 673 (Figure 1a). The characteristic GXSXG motif is located between aa 381 and aa 385, while the catalytic aspartate of the dyad is located at aa 531. 3D modelling of PNPLA1 was done using the I-TASSER server based on the crystal structure of PDB hit 6AUN (Malley et al., 2018), a human calcium-independent phospholipase $A_2\beta$ with cytosolic localisation that is involved in diverse biological processes including fat catabolism, cell differentiation and phospholipid remodelling (reviewed in Barbour & Ramanadham, 2017; Figure S1A). The model shows the serine (aa 383) and aspartate (aa 531), representing the catalytic dyad, being in close spatial proximity within the C-terminal catalytic domain. Phylogenetic analysis of PNPLA1 and related proteins from other plasmodia identified the highest identities with the homologous proteins of *P. ovale* and *P. malariae*, while the highest diversity was found in the PNPLA1 homolog of *P. berghei* (Figure S1b). All of the plasmodial PNPLA1 homologs share the GXSXG motif and the catalytic aspartate; the homologs of *P. vivax* and *P. knowlesi* further exhibit N-terminal extensions (Figure S2).

Diagnostic reverse transcriptase (RT)-PCR was performed to investigate expression of *pnpla1* in the *P. falciparum* blood stages and demonstrated transcripts in the ring and trophozoite stages and in schizonts. Similar transcript levels were detected in immature (Stage II–IV) and mature (Stage V) gametocytes as well as in gametocytes at 15' post-activation (p.a.; Figure S3a). Transcript analysis of the

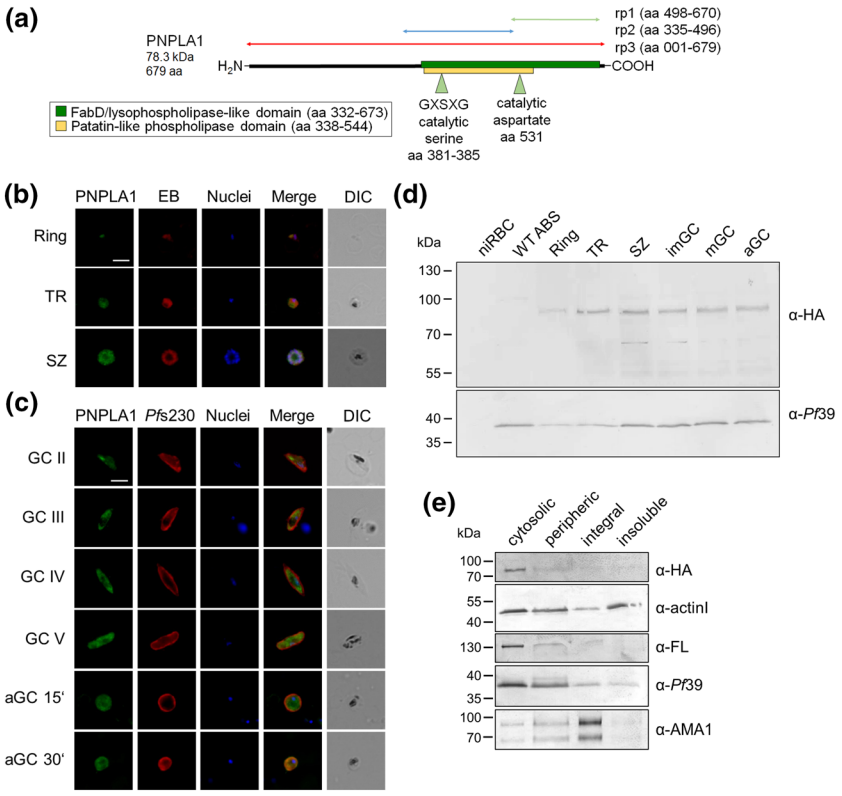

FIGURE 1 PNPLA1 is expressed in the asexual blood and gametocyte stages of *P. falciparum*. (a) Schematic depicting the domain architecture of PNPLA1. The FabD/lysophospholipase-like domain (green) and the patatin-like phospholipase domain (yellow), the catalytic serine lipase motif GXSXG and the catalytic aspartate, both constituting the serine-aspartate dyad, are highlighted. Regions used for generation of recombinant proteins (rp) are indicated. aa, amino acids; FabD, fatty acid binding domain; G, glycine; S, serine. (b, c) PNPLA1 localisation to the blood stage cytosol. Rings, trophozoites (TR) and schizonts (SZ) (b) or gametocytes (GCII-GCV) and activated gametocytes (aGC; at 15 and 30 min p.a.) (c) of WT were immunolabelled with mouse anti-PNPLA1rp1 antisera (green). The asexual blood stages were stained with EB; the gametocytes were counterlabelled with rabbit anti-*Pfs*230 sera (red). The parasite nuclei were highlighted by Hoechst 33342 nuclear stain (blue). DIC, differential interference contrast. Bar, 5 μm. (d) PNPLA1-HA expression in blood stage parasites. WB of lysates from rings, trophozoites (TR), schizonts (SZ), immature (imGC), mature (mGC) and activated gametocytes (aGC, 30 min p.a.) of the (untreated) PNPLA1-KD line, using rabbit anti-HA antibody, detected PNPLA1-HA at the expected size of ~78 kDa. Lysates of mixed WT asexual blood stages (WT ABS) and non-infected RBCs (niRBCs) were used as negative controls; equal loading was confirmed using polyclonal mouse antisera against *Pf*39 (~39 kDa). (e) Subcellular localisation of PNPLA1-HA. Lysates of mixed asexual blood stages of the (untreated) PNPLA1-KD line were used to extract soluble, integral, peripheric and insoluble protein fractions. Samples were immunoblotted with rabbit anti-HA antibodies to detect PNPLA1-HA (~82 kDa); immunoblotting with mouse antisera against actin I (~42 kDa), falcilysin (~138 kDa), *Pf*39 (~39 kDa) and AMA1 (~66 and 88 kDa) were used for fraction controls. Results (b–e) are representative of 2–3 independent experiments

housekeeping gene *aldolase* was used as a loading control, and purity of the asexual blood stage and gametocyte samples was demonstrated by amplification of transcripts for the asexual blood stage-specific gene *pfama1* (apical membrane antigen 1; Peterson et al., 1989) and for the gametocyte-specific gene *pfccp2* (LCCL-domain protein 2; Pradel et al., 2004). The cDNA preparations lacking the reverse transcriptase were used to verify that samples were devoid of gDNA (Figure S3a).

Mouse antisera were generated against two recombinant PNPLA1 peptides comprising parts of the lysophospholipase and the patatin-like phospholipase domain (PNPLA1rp1 and PNPLA1rp2, respectively; see Figure 1a) to be used for protein expression analysis. In addition, a full-length recombinant protein was used in Western blot (WB) analyses to confirm the specificity of PNPLA1rp1 and PNPLA1rp2 (Figure S3b). Indirect immunofluorescence assays (IFAs), using either of the two antisera, revealed that PNPLA1 was abundantly expressed in the asexual blood stages, where it localised to the cytosol (Figures 1b and S4a). PNPLA1 was further detected in the cytosol of gametocytes during development and at 15 and 30 min p.a. (Figures 1c and S4b). Counterlabelling with antibodies either directed against *Pfs*25, a female-specific epidermal growth factor domain protein, or against *Pfs*230, a cysteine-rich protein present in both male and female gametocytes (reviewed in Pradel, 2007), demonstrated that PNPLA1 is present in both male and female gametocytes and thus expressed in a gender-independent pattern (Figure S4c). When sera from non-immunised mice (NMS) were used in the IFAs as a negative control, no labelling was detectable in either asexual blood stages or gametocytes (Figure S4d).

2.2 | PNPLA1-deficient blood stage parasites are impaired in gametocyte induction

We generated two PNPLA1-deficient lines for functional analyses. First, *P. falciparum* parasites lacking the *pnpla1*-encoding gene were generated via single cross-over homologous recombination, using the vector pCAM-BSD (Figure S5a). Two clonal lines (A12 and C11) of the PNPLA1-knock out (KO) were isolated and successful integration of the plasmid into the genome was verified by diagnostic PCR and by sequencing of the integration loci (Figures S5b and S6). The absence of the protein in PNPLA1-KO schizonts of both lines compared to the wildtype (WT) was subsequently demonstrated by IFA (Figure S5c). Similarly, WB using the mouse anti-PNPLA1rp1 antisera, could detect a PNPLA1-positive protein band with the expected molecular weight in blood stage lysates of the WT, but not in lysates of the two PNPLA1-KO lines (Figure S5d).

In addition, we generated a conditional PNPLA1-knock down (KD) line (using the pARL-HA-*glmS* vector), by fusing the sequences coding for a hemagglutinin A (HA) tag and for the *glmS* element to the 3′-region of *pnpla1* (Figure S7a). In the PNPLA1-KD, the *pnpla1* mRNA is expressed under the control of the *glmS* ribozyme (Prommana et al., 2013), which catalyses its own cleavage in the presence of glucosamine (GlcN) and thus triggers degradation of the *pnpla1* mRNA. Vector integration was confirmed by diagnostic PCR and sequencing of the integration sites (Figures S7a,b and S8). Immunolabelling with an anti-HA antibody confirmed the synthesis of a HA-tagged PNPLA1 fusion protein in the untreated PNPLA1-KD line, while no signal was detected in WT (Figure S7c). To prove the conditional down-regulation of PNPLA1 synthesis, asexual blood stage parasites were treated with 2.5 mM GlcN for 72 hr. Upon GlcN addition, PNPLA1 levels were significantly reduced to 40.00 ± 13.4% compared to the untreated control (Figure S7d,e).

The (untreated) PNPLA1-KD line was used for in-depth expression analysis. IFAs, using anti-HA antibody, verified a cytosolic localisation of PNPLA1-HA in the asexual blood stages and the gametocytes, while WT blood stage parasites did not show any labelling (Figure S9). In addition, immunoblotting with the anti-HA antibody detected PNPLA1-HA running with a molecular weight of 82 kDa in the PNPLA1-KD lysates, but not the WT and RBC lysates, and confirmed protein expression in the asexual blood stages as well in gametocytes during development and following activation (Figure 1d). Subcellular fractioning further demonstrated that PNPLA1-HA locates to the cytosolic fraction of the blood stage parasite, while the protein was absent in the peripheric, the integral and the insoluble factions (Figure 1e). Immunoblotting with antibodies against the cytoskeletal element actin 1 (Ngwa et al., 2013; reviewed in Baum, Gilberger, Frischknecht, & Meissner, 2008), the cytosolic protease falcilysin (Weißbach, Golzmann, Bennink, Pradel, & Julius Ngwa, 2017), the endoplasmic reticulum-associated protein *Pf*39 (Simon et al., 2009) and the transmembrane protein AMA1 (Boes et al., 2015; Peterson et al., 1989) were used as fractionation controls.

Initial phenotype analyses of the two PNPLA1-KO lines showed that intraerythrocytic development of the asexual blood stages was normal compared to WT and no differences in parasitemia over a period of 120 hr as well as in blood stage morphology and progression and in the numbers of merozoites formed per schizont were observed (Figures 2a–c and S10a). Furthermore, no significant differences in the exflagellation behaviour as well as in the formation of macrogametes and zygotes following *in vitro* activation of the PNPLA1-KO gametocytes was seen (Figure 2d). When the gametocytemia was compared between the PNPLA1-KO lines and the WT over a period of 14 days, however, significant reductions in the numbers of gametocytes were documented (Figure 2e). In addition, gametocyte maturation was significantly delayed in the PNPLA1-KO lines compared to the WT, when the development of the gametocyte stages II–V was followed over a period of 2 weeks (Figures 2e and Figure S10b,c).

To investigate the effect of PNPLA1-deficiency on gametocytes in more detail, we used the PNPLA1-KD line in the follow-up experiments. We confirmed that reduced PNPLA1 synthesis did not lead to any differences in parasitemia over a period of 120 hr as well as in blood stage morphology and progression, when these were treated or not treated with GlcN (Figures 3a and S11a,b). The low PNPLA1 levels, however, significantly reduced gametocyte numbers in the GlcN-treated PNPLA1-KD line, when this line was compared to untreated PNPLA1-KD parasites and treated or untreated WT parasites (Figure 3b). To determine, if the PNPLA1-deficiency effects gametocyte induction or rather gametocyte development, we treated the blood stages with GlcN either before or after addition of lysed RBCs, which act as gametocytogenesis-promoting factor. We observed that PNPLA1 down-regulation prior to gametocyte induction resulted in significantly reduced gametocyte numbers, while PNPLA1 down-regulation after gametocyte induction had no effect on gametocyte development (Figure 3c). Untreated PNPLA1-KD parasites as well as GlcN-treated and untreated WT were used for controls in these experiments.

2.3 | PNPLA1 deficiency counteracts gametocyte induction by serum-free medium

In a recent study, Brancucci et al. (2017) reported that serum-free cell culture medium (-SerM), which only contained the minimally required fatty acid species C16:0 and C18:1 necessary for the growth of the *P. falciparum* blood stages (Mi-Ichi, Kano, & Mitamura, 2007; Mi-Ichi, Kita, & Mitamura, 2006), promotes sexual commitment. This effect could be reverted by addition of lysoPC to the medium. We thus repeated the above experiments and induced gametocyte formation by incubation of the blood stage parasites in -SerM. We confirmed that in the WT treatment with -SerM resulted in an increased formation of gametocytes compared to medium supplemented with lysoPC, choline or human serum (Figure 4a). The two PNPLA1-KO lines, however, formed significantly reduced numbers of gametocytes, when induced with -SerM medium compared to the WT (Figure 4a). Similarly, the PNPLA1-KD line did not produce increased gametocyte numbers in response to -SerM, when treated with GlcN prior to gametocyte induction, while the untreated PNPLA1-KD line formed higher

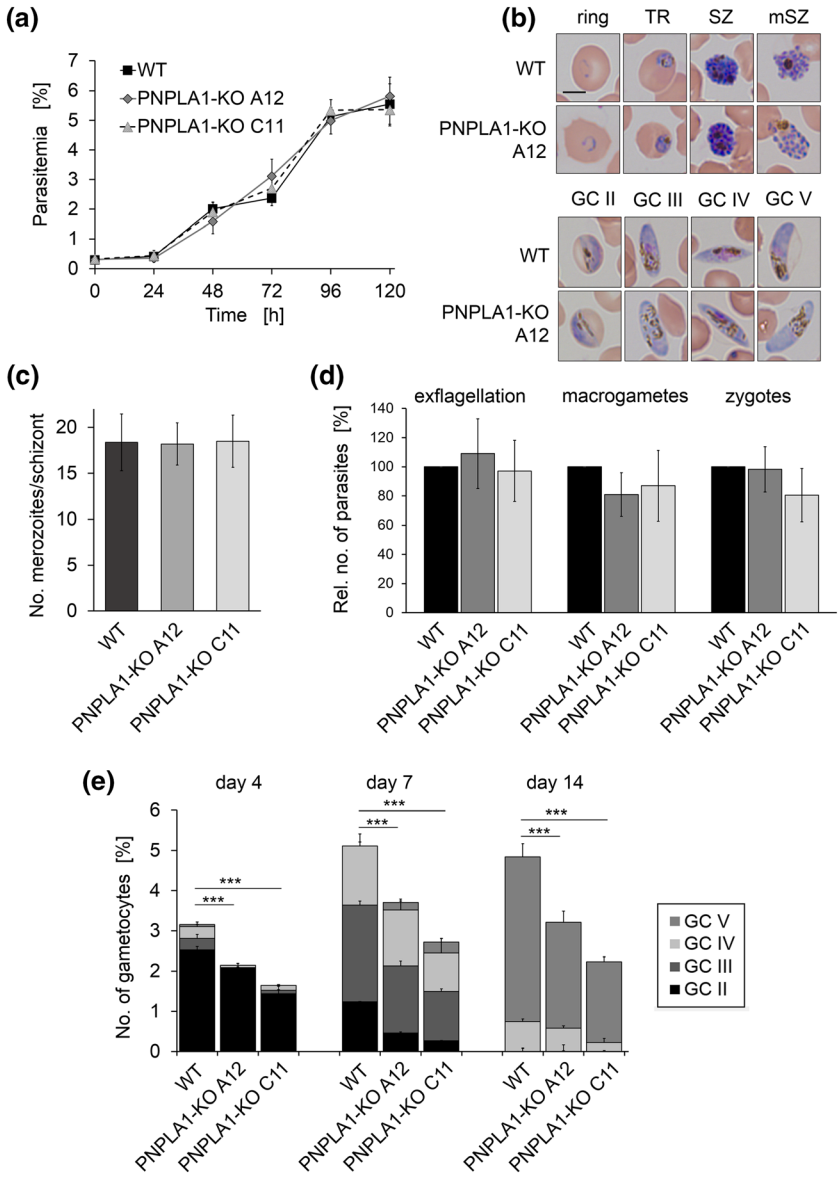

FIGURE 2 PNPLA1-KO parasites are impaired in gametocytogenesis. (a) Asexual blood stage replication of the PNPLA1-KO. Synchronised ring stage cultures of WT and PNPLA1-KO A12 and C11 with a starting parasitemia of 0.25% were maintained in cell culture medium and parasitemia was followed via Giemsa smears over a time-period of 0–120 hr. The experiment was performed in triplicate (mean ± SD). (b) Morphology of the PNPLA1-KO blood stages. The morphology was demonstrated via Giemsa staining of asexual blood stages and gametocytes of the PNPLA1-KO A12 line and WT. TR, trophozoites; SZ, schizonts; mSZ, mature schizonts; GC, gametocytes II–V. Bar, 5 μm. (c) Merozoite formation in PNPLA1-KO schizonts. Schizonts were stained with EB and merozoites were highlighted by Hoechst 33342 nuclear stain. Merozoite numbers were counted in triplicate for 75 schizonts per parasite line. Data are shown as mean ± SD. (d) Gametogenesis of the PNPLA1-KO. Mature WT and PNPLA1-KO A12 and C11 gametocytes were activated *in vitro*. Samples were taken at 15 min p.a. (exflagellation centres), 30 min p.a. (macrogametes) and 6 hr p.a. (zygotes). Exflagellation centres were counted in 30 optical fields for four times using light microscopy. Zygotes and macrogametes were immunolabelled with anti-*Pfs*25 antibody and counted in 30 optical fields in triplicate. Results are shown as mean ± SD (WT set to 100%). (e) Gametocyte development of the PNPLA1-KO. Synchronised ring stage cultures of WT and the PNPLA1-KO lines A12 and C11 with a starting parasitemia of 2.0% were grown in cell culture medium and numbers of gametocytes were followed via Giemsa smears over a time-period of 14 days. The experiment was performed in triplicate (mean ± SD). ***$p \leq 0.001$ (one-way ANOVA with post hoc Bonferroni multiple comparison test). Results data (a–e) are representative of 3–5 independent experiments

gametocyte numbers in -SerM compared to medium supplemented with lysoPC or choline (Figure 4b).

Brancucci et al. (2017) further described that lysoPC-depletion triggers an immediate transcriptional upregulation of a variety of genes important for gametocytogenesis. The genes, among others, include the ones encoding the transcriptional regulators of sexual commitment *ap2-g* (Brancucci et al., 2017; Kafsack et al., 2014; Sinha et al., 2014) and the gametocytogenesis modulator *gdv1* (Brancucci

et al., 2017; Eksi et al., 2012; Filarsky et al., 2018; Usui et al., 2019). Furthermore, genes coding for enzymes that are known to be involved in the utilisation of ethanolamine to generate PC were up-regulated (Bobenchik et al., 2010; Brancucci et al., 2017; Pessi, Choi, Reynolds, Voelker, & Mamoun, 2005; Pessi, Kociubinski, & Mamoun, 2004). We chose eight of these genes and investigated their transcriptional levels of the genes by real-time RT-PCR at 46 ± 2 h.p.i. (hours post-invasion) following induction with -SerM compared to incubation with -SerM supplemented with lysoPC. For the eight genes, a twofold to sixfold transcriptional upregulation could be observed in the -SerM-cultivated WT (Figure S12a,b). A similar transcriptional up-regulation was seen in the PNPLA1-KO lines A12 and C11, but the fold-changes were partially decreased. For the transcription factor AP2-G, which is responsible for activating expression of gametocyte-specific genes at the onset of sexual commitment (Kafsack et al., 2014; Sinha et al., 2014) and the phos-pho-ethanolamine N-methyltransferase PMT that catalyses the conversion of phos-pho-ethanolamine into phosphocholine to compensate for the lack of PC-precursors (Brancucci et al., 2017), significantly reduced transcript levels compared to the -SerM-induced WT control were observed.

In a next step, the effect of commercial PLA_2 inhibitors on gametocyte induction was tested. First, the antimalarial effect of the four inhibitors 4-bromophenacyl bromide (4-BPB), bromoenol lactone, ASB14780 and N-(p-amylcinnamoyl) anthranilic acid on erythrocytic replication was investigated, using the Malstat assay. The highest antimalarial effect was detected for 4-BPB with an IC_{50} value of 5.6 ± 0.82 μM (Table 1). This concentration was used to treat asexual blood stages when inducing gametocytes by -SerM. When the asexual blood stages were treated with 4-BPB, significantly reduced gametocyte numbers were observed in the WT upon -SerM incubation compared the untreated WT and the solvent control (Figure 4c). In the two PNPLA1-KO lines, however, no significant differences were observed in 4-BPB-treated parasites compared to the controls. Similarly, in the PNPLA1-KD not treated with GlcN, exposure to 4-BPB resulted in less gametocyte numbers following induction with -SerM compared to WT and solvent controls, while no such effect could be observed, when the inhibitor-exposed PNPLA1-KD line was treated with GlcN prior to induction (Figure S12c). 4-BPB treatment, however, had no significant effect on gametocyte maturation and gametocyte stage progression, when added at the IC_{50} concentration to early stage II gametocytes, compared to the solvent or chloroquine-treated controls (Figure S12d,e). Epoxomicin used for positive control (Aminake et al., 2011; Czesny, Goshu, Cook, & Williamson, 2009) killed the gametocytes.

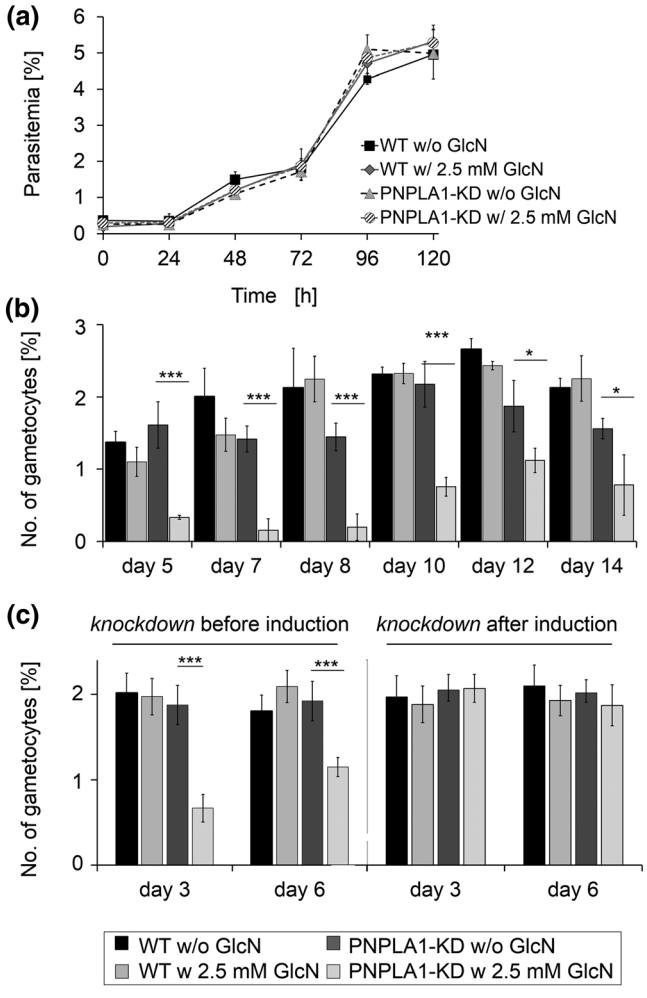

FIGURE 3 PNPLA1-KD parasites are impaired in gametocyte induction. (a) Asexual blood stage replication of the PNPLA1-KD. Synchronised ring stage cultures of WT and the PNPLA1-KD with a starting parasitemia of 0.25% were maintained in cell culture medium supplemented with 2.5 mM GlcN to knockdown PNPLA1 protein expression and parasitemia was followed via Giemsa smears over a time-period of 0–120 hr. Untreated (without GlcN) cultures and WT were used as controls. The experiment was performed in triplicate (mean ± SD). (b) Gametocyte formation in the PNPLA1-KD. Synchronised ring stage cultures of WT and the PNPLA1-KD with a starting parasitemia of 2.0% were grown in cell culture medium supplemented with 2.5 mM GlcN and numbers of gametocytes were followed via Giemsa smears over a time-period of 14 days. Untreated (without GlcN) cultures and WT either without or treatment with 2.5 mM GlcN were used as controls. The experiment was performed in triplicate (mean ± SD). ***$p \leq 0.001$ (one-way ANOVA with post hoc Bonferroni multiple comparison test). (c) Gametocyte induction and maturation of the PNPLA1-KD. Synchronised ring stage cultures of WT and the PNPLA1-KD with a starting parasitemia of 2.0% were grown in cell culture medium until a parasitemia of 10.0% ring stages was reached. For gametocyte induction, cultures were exposed to lysed RBCs for 24 hr, washed with cell culture medium and further grown in cell culture medium supplemented with 50 mM GlcNac to kill the asexual blood stages. Cultures were treated with 2.5 mM GlcN to knockdown PNPLA1 protein expression either before or after removal of the gametocytogenesis-promoting lysed RBCs. Numbers of gametocytes were determined via Giemsa smears on day 3 and 6 p.g.i. The experiment was performed in triplicate (mean ± *SD*). ***$p \leq 0.001$ (one-way ANOVA with post hoc Bonferroni multiple comparison test). Results (a–c) are representative of 2–3 independent experiments

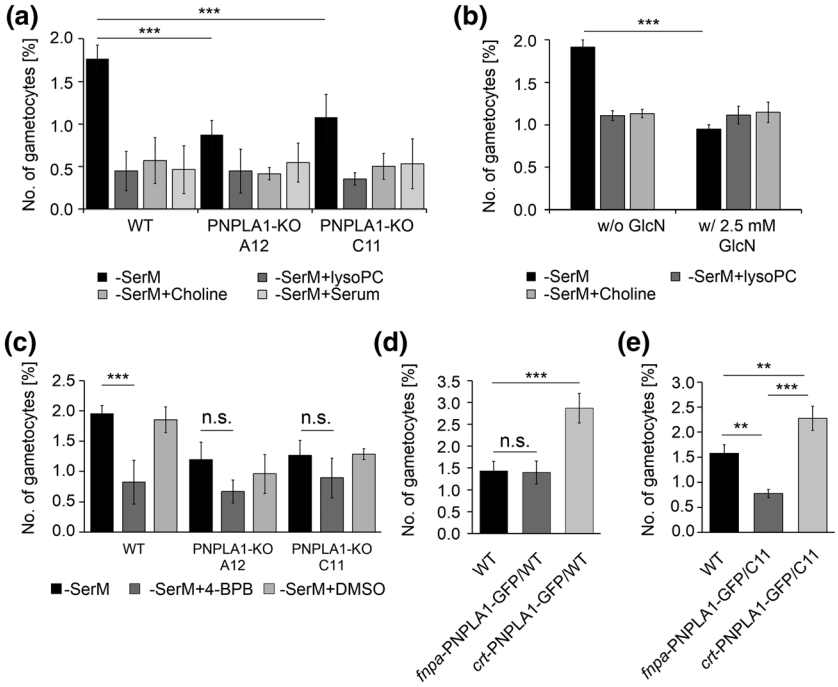

FIGURE 4 PNPLA1 levels effect gametocyte induction rates. (a, b) Gametocyte induction in the PNPLA1-deficient lines. Synchronised parasite cultures of WT and the PNPLA1-KO lines A12 and C11 (a) or the PNPLA1-KD line without or following treatment with 2.5 mM GlcN (b) were induced with -SerM at 28 ± 2 h.p.i. for 22 hr and further grown in cell culture medium supplemented with 50 mM GlcNac for 5 days to kill the asexual parasites. For control, -SerM was supplemented with 20 μM lysoPC, with 300 μM choline and 11.1 mM glucose or with 10% v/v HIS. Numbers of gametocytes were determined via Giemsa smears on day 5 p.g.i. The experiments (a, b) were performed in triplicate (mean ± *SD*). (*c*) Effect of the PLA_2 inhibitor 4-BPB on gametocyte induction. Synchronised WT and the PNPLA1-KO lines A12 and C11 treated with -SerM supplemented with 4-BPB at IC_{50} concentration at 28 ± 2 h.p.i. for 22 hr and further grown in cell culture medium supplemented with 50 mM GlcNac for 5 days to kill the asexual parasites. Parasites cultivated in medium with or without 1% v/v DMSO were used as control. (d, e) Effect of PNPLA1 overexpression on gametocyte development. Synchronised parasite cultures of WT and the two lines *fnpa*-PNPLA1-GFP/WT and *crt*-PNPLA1-GFP/WT (d) or the two lines *fnpa*-PNPLA1-GFP/C11 and *crt*-PNPLA1-GFP/C11 were treated with -SerM at 28 ± 2 h.p.i. for 22 hr and further grown in cell culture medium supplemented with 50 mM GlcNac for 5 days to kill the asexual parasites. Numbers of gametocytes were determined via Giemsa smears on day 5 p.g.i. The experiments (d, e) were performed in triplicate (mean ± *SD*). $^{**}p \leq 0.01$; $^{***}p \leq 0.001$ (one-way ANOVA with post hoc Bonferroni multiple comparison test). Results (a–e) are representative of three independent experiments

2.4 | PNPLA1 overexpression promotes gametocyte induction

We also investigated the effect of PNPLA1 overexpression on gametocyte induction. The sequence for full-length PNPLA1 was cloned into the vector pARLII-GFP, which was driven either under the control of the *crt* (chloroquine-resistance transporter) promoter (Külzer et al., 2010; Przyborski et al., 2005; Spork et al., 2009), which is predominantly active in the asexual blood stages, or the gametocyte-specific *fnpa* promoter, which is exclusively active in the sexual blood stages (Bennink et al., 2018; Pradel et al., 2004; Figure S13a). WT parasites were transfected and the presence of the plasmids in the transfectant lines was verified by diagnostic PCR; purified plasmid DNA was used for control (Figure S13b). Live imaging showed that the *crt* promoter allowed the episomal expression of PNPLA1 in the transfected asexual blood stages (line *crt*-PNPLA1-GFP/WT), while the protein was expressed only in transfected gametocytes when controlled by the *fnpa* promoter (line *fnpa*-PNPLA1-GFP/WT; Figure S13c). WT parasites did show GFP expression (Figure S13d). Asexual blood stages of the transfectant lines *crt*-PNPLA1-GFP/WT and *fnpa*-PNPLA1-GFP/WT were subsequently induced by -SerM, which resulted in significantly increased gametocyte numbers in the *crt*-PNPLA1-GFP/WT line at day 5 post-gametocyte induction (p.g.i.) compared to the WT and *fnpa*-PNPLA1-GFP/WT (Figure 4d). No differences in the morphology of the asexual and sexual blood stages, though, were

TABLE 1 Antimalarial activities of PLA_2 inhibitors

Inhibitor	IC_{50} (μM)
4-Bromophenacyl bromide	5.6 ± 0.82
Bromoenol lactone	85.9 ± 11.29
ASB 14780	56.9 ± 8.85
N-(*p*-amylcinnamoyl) anthranilic acid	9.8 ± 1.81
Chloroquine	0.012 ± 0.0019

observed in lines *crt*-PNPLA1-GFP/WT and *fnpa*-PNPLA1-GFP/WT compared to WT (Figure S14).

To prove the direct link between PNPLA1-deficiency and impaired gametocyte induction, we further conducted a complementation assay. The PNPLA1-KO line C11 was transfected with either of the above two plasmids. The presence of the plasmids in the PNPLA-1 KO C11 transfectant line was verified by diagnostic PCR; purified plasmid DNA was used for control (Figure S15a). Subsequent WB analyses demonstrated the presence of PNPLA1-GFP in the lysates of asexual blood stages, but not of gametocytes, when the C11 line was transfected with plasmid pARLII-*crt-pnpla1-gfp*, while lysates of gametocytes, but not asexual blood stages were positive for PNPLA1-GFP, when the C11 line was transfected with plasmid pARLII-*fnpa-pnpla1-gfp* (Figure S15b). Lysates of WT and non-infected RBCs were used as negative controls in the WB experiment. Asexual blood stages of the transfectant lines *crt*-PNPLA1-GFP/C11 and *fnpa*-PNPLA1-GFP/C11 were then induced by -SerM. Gametocyte induction resulted in significantly increased gametocyte numbers in the *crt*-PNPLA1-GFP/C11 line at day 5 p.g.i. compared to *fnpa*-PNPLA1-GFP/C11, which were even higher than in the WT (Figure 4e), indicating that the loss-of-function phenotype of the PNPLA1-KO was reverted by episomal expression of PNPLA1.

2.5 | PNPLA1-deficiency results in an overall increase of major phospholipids

In a last set of experiments, we wanted to find out, whether the parasite phospholipid composition was altered in the blood stages of the two PNPLA1-KO lines. Synchronised ring stages of WT and the PNPLA1-KO lines A12 and C11 were liberated from the enveloping RBCs and total lipids were extracted. RBC lysis was controlled by Giemsa smears (Figure S16) and the purity of the synchronised ring stages was verified by amplification of *rex1* (ring-exported protein 1; Hawthorne et al., 2004) and *sbp1* (skeleton-binding protein 1; Blisnick et al., 2000) transcripts via diagnostic and real-time RT-PCR. Transcript amplification of the gametocyte-specific gene *ccp2* was used for negative control and transcript amplification of the house-keeping gene *gapdh* was used for positive control in the experiments, while *pnpla1* transcript amplification served as PNPLA1-KO control (-Figure S17a,b). The lipid extracts were mixed with an internal lipid standard mix (LIPDOMIX standard, Avanti). Each lipid class was separated by high-performance thin layer chromatography and then extracted from the silica gel. Total fatty acids from each lipid class were methanolised to fatty acid methyl ester and then quantified by GC-MS.

The lipidomics analyses revealed that both the total fatty acid and phospholipid levels of the two PNPLA1-KO lines were slightly higher compared to the WT (Figure 5a,b). Particularly, the absolute PC levels were significantly increased in the two PNPLA1-KO lines in comparison to the WT (Figure 5b). This did not alter the overall phospholipid composition, though (Figure 5c), probably for the parasite to keep its membrane integrity. Solely for the relative lysobisphosphatidic acid (LBPA) levels, a decrease in the PNPLA1-KO lines compared to WT could be observed (Figure 5b,c). The lysoPC content in the different lines was below detection level (data not shown).

3 | DISCUSSION

During infection with *P. falciparum*, gametocytes begin to develop ~1 week after the appearance of parasites in the human blood. A small proportion of committed parasites leaves the asexual blood stage cycle and enters the sexual pathway on a continuous basis, an event probably driven by endogenous factors. Previously, the transcription factor AP2-G was identified as a key regulator of sexual commitment (Kafsack et al., 2014; Sinha et al., 2014). During intraerythrocytic replication, the *ap2-g* locus is silenced by histone acetylation and methylation and silencing further involves chromatin condensation mediated by heterochromatin protein HP1 (Coleman et al., 2014; Brancucci et al., 2014; reviewed in Josling, Williamson, & Llinás, 2018). During sexual commitment, though, the *ap2-g* locus is activated by HP1 release and chromatin decondensation, which among others involves the histone deacetylase Hda2 and the modulator GDV1 (gametocyte development protein 1; Coleman et al., 2014; Filarsky et al., 2018; Usui et al., 2019; reviewed in Rea, Le Roch, & Tewari, 2018). Once synthesised, AP2-G, regulates the expression of a variety of gametocyte-specific genes (Brancucci et al., 2014; Poran et al., 2017).

The sexual commitment rate is upregulated in response to environmental stress signals, including parasite density, anaemia or drug treatment (e.g. Usui et al., 2019; reviewed in Alano, 2007; Kuehn & Pradel, 2010). Increasing data suggest that the lack of phospholipid precursors in the human serum augments gametocyte production. Particularly, low serum levels of lysoPC, which was recently shown to act as the main exogenous precursor of PC, cause the blood stage parasites to enter the sexual pathway, among others initiated by the upregulation of *ap2-g* expression (Brancucci et al., 2017). Despite previous assumptions that choline is acquired from serum, new data indicate that the majority of choline to be incorporated in PC is generated from serum-imported lysoPC (Wein et al., 2018; Figure 6).

RBCs infected either with trophozoites or gametocytes have a roughly sixfold higher phospholipid content compared to non-infected RBCs. The proportion of PC levels, though, are lower in gametocytes than in trophozoites and decrease further during maturation (Tran et al., 2016). Under normal serum conditions, PC is generated de novo from precursors by the cytidine diphosphate (CDP)-choline (Kennedy) pathway (reviewed in Tischer, Pradel, Ohlsen, & Holzgrabe, 2012; Flammersfeld et al., 2018). In the absence of lysoPC in the serum, however, PC is mainly synthesised via triple-methylation of phos-phoethanolamine using ethanolamine (from serum) or serine (from hemoglobin) as external precursors (Figure 6). This pathway involves the activity of PMT and parasite lines deficient of PMT die in serum lacking these precursors (Wein et al., 2018). This alternative route of PC synthesis via the PMT pathway appears to be upregulated during sexual commitment due to lysoPC depletion, as shown by increased transcript synthesis of PMT and S-adenosylmethionine (SAM) synthetase

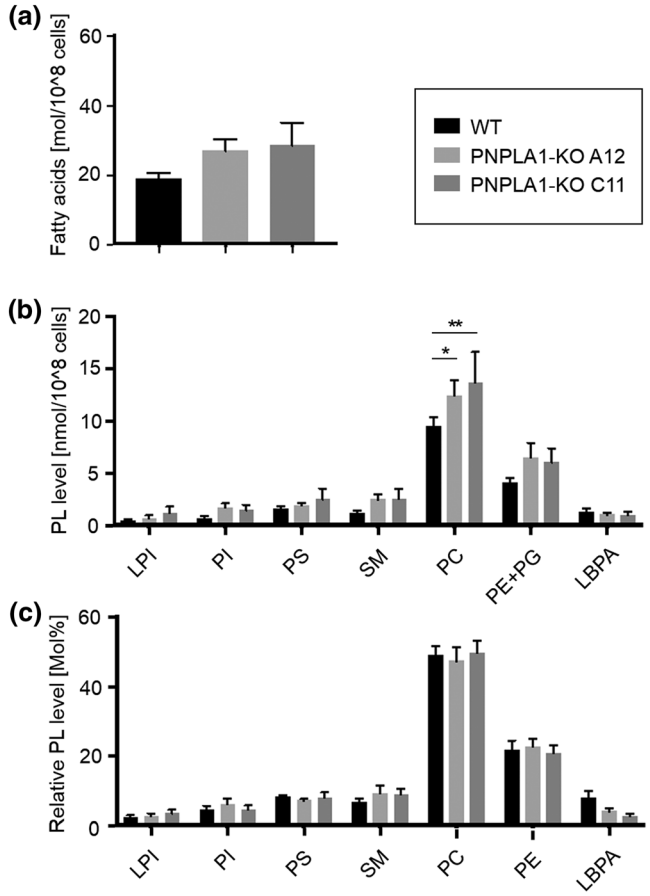

FIGURE 5 PNPLA1-KO parasites exhibit altered phospholipid levels. (a) Fatty acid content of PNPLA1-KO parasites. Lipids were extracted from synchronised ring stages of WT and the PNPLA1-KO lines A12 and C11 and employed to lipidomics. The absolute fatty acid levels were compared after the normalisation to parasite number of 10^8. (b) Phospholipid content of PNPLA1-KO parasites. The absolute levels of selected phospholipids were compared following normalisation to 10^8 parasites. Statistical analysis was performed with GraphPad Prism 5 software using two-way ANOVA analysis. *p* value is shown as $*p \leq 0.05$; $**p \leq 0.01$. (c) Phospholipid composition of PNPLA1-KO parasites. The relative phospholipid levels are shown as Mol%. LBPA, lysobisphosphatidic acid; LPI, lysophosphatidylinositol; PC, phosphatidylcholine; PE, phosphatidylethanolamine; PG, phosphatidylglycerol; PI, phosphatidylinositol; PL, phospholipid; PS, phosphatidylserine; SM, sphingomyelin. The lipidomics analysis was performed using four biological replicates of each line

under these conditions (Brancucci et al., 2018, 2017). While to date the link between low lysoPC availability and sexual commitment is not clear, it has been postulated that under reduced lysoPC conditions, the parasites need to utilize the methyl donor SAM to generate PC, and in consequence less SAM could be used to repress the *ap2-g* locus via histone methylation (Llinás, 2017).

While these data demonstrate the high sensitivity of the plasmodial blood stages to the availability of phospholipids, we now show that PNPLA1 of the parasite is involved in the PC synthesis-dependent shift from asexual blood stage replication to gametocyte development. PNPLA1 is a cytosolic PLA_2 of the asexual blood and gametocyte stages with a particular role in gametocyte induction. Asexual blood stage parasites lacking PNPLA1 due to conventional gene-KO or conditional gene-KD, are less responsive to modulators of sexual commitment, including lysoPC deficiency. This loss-of-function phenotype can be mimicked by the PLA_2 inhibitor 4-BPB. In contrast, overexpression of PNPLA1 both in WT or in PNPLA1-KO parasites leads to higher gametocytemia and the combined data point to a direct link between PNPLA1 activity and gametocyte induction.

The lack of PNPLA1 further results in a deregulation of the major phospholipid biosynthesis pathway in the asexual blood stages. Lipidomics indicated partially increased levels of phospholipids and particularly measured higher absolute PC levels in the absence of PNPLA1. Noteworthy, PLA_2 activities were predicted to be important for two reactions of this pathway; that is, the degradation of PC to lysoPC and the degradation of PE to lysoPE (see mpmp.huji.ac.il). In consequence, the loss of PLA_2 activity would evidently result in an accumulation of PC, PE and PS, and could also lead to an increased conversion of PC into SM (Figure 6). Such changes in phospholipid compositions have had been observed in the PNPLA1-KO lines.

PNPLA1 is one of four PNPLAs identified in *P. falciparum*, and, to date, only for PNPLA1 functional data were collected. In a recent publication, Singh et al. (2019) reported a role for PNPLA1 (termed PATPL1 in this study) in malaria transmission. In accord with our data, the authors detected PNPLA1/ PATPL1 in the cytosol of the asexual and sexual blood stages of *P. falciparum*. However, the authors described an effect of PNPLA1/PATPL1-deficiency due to conditional gene-KO or protein-KD in gametogenesis rather than gametocyte induction and suggested an involvement of PNPLA1/PATPL1 in plasma membrane disruption during RBC egress. In contrast to these findings, we were not able to detect any significant effect of PNPLA1-deficiency on exflagellation or gamete formation in multiple independently performed experiments. Noteworthy, we reported a delayed gametocyte maturation period for gametocytes in the absence of PNPLA1. Such delayed maturation may eventually result in defective gametogenesis, if not fully matured gametocytes have been used in the exflagellation and RBC egress assays.

PNPLAs can also be found in the Apicomplexan parasite *Toxoplasma gondii*; here, three of the roughly six annotated PNPLAs have meanwhile been functionally characterised. The two PNPLAs *Tg*PL1 and *Tg*PLA_2 localize to vesicles and are discharged upon immune stress and during invasion, while *Tg*PL2 is crucial for apicoplast integrity (Cassaing et al., 2000; Lévêque et al., 2017; Mordue, Scott-Weathers, Tobin, & Knoll, 2007; reviewed in Tobin & Knoll, 2012). In addition, in other eukaryotes important functions were assigned to PNPLAs. For example, PNPLAs are usually synthesised upon virus infection to generate signalling molecules that induce programmed cell death of the infected tissue in tobacco plants (e.g. Dhondt, Geoffroy, Stelmach, Legrand, & Heitz, 2000; Dhondt, Gouzerh, Muller, Legrand, & Heitz, 2002; reviewed in Ryu, 2004). Mammalian PNPLAs, in contrast, are mostly used in lipid turnover, for example, triglyceride

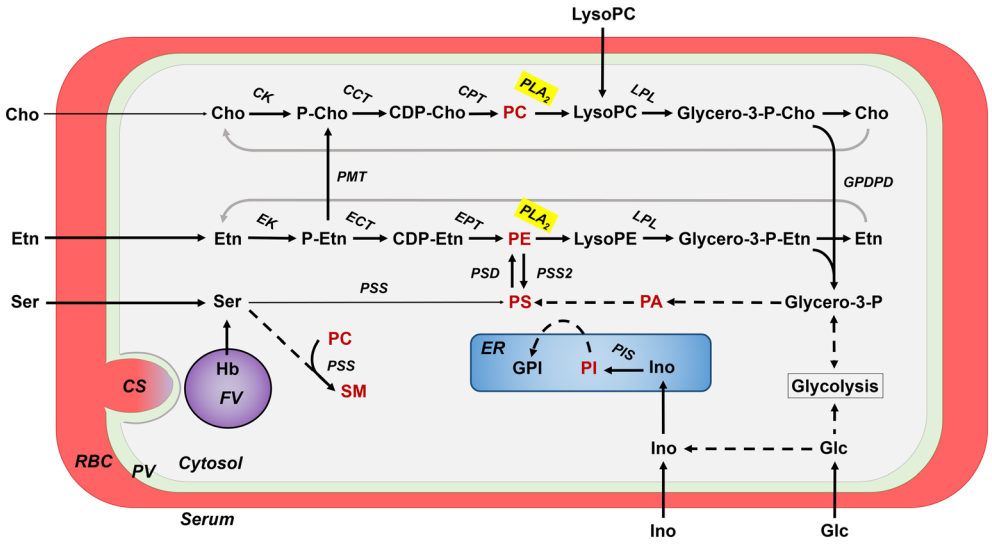

FIGURE 6 Schematic depicting the main phospholipid synthesis pathways of the *P. falciparum* blood stages. CCT, choline-phosphate cytidyltransferase; CPT, cholinephosphotransferase; CDP-Cho, cytidine diphosphate choline; CDP-Etn, cytidine diphosphate ethanolamine; Cho, choline; CK, choline kinase; CS, cytostome; ECT, ethanolamine-phosphate cytidyltransferase; EPT, ethanolaminephosphotransferase; ER, endoplasmatic reticulum; Etn, ethanolamine; FV, food vacuole; Glc, glucose; Glycero-3-P, glycerol-3-phosphate; GPDPD, glycerophosphodiester phosphodiesterase; GPI, glycosylphosphatidylinositol; Hb, hemoglobin; Ino, inositol; LPL, lysophospholipase; lysoPC, lysophosphatidylcholine; lysoPE, lysophosphatidylethanolamine; PA, phosphatidic acid; PC, phosphatidylcholine; P-Cho, phosphocholine; PE, phosphatidylethanolamine; P-Etn, phos-pho-ethanolamine; PI, phosphatidylinositol; PIS, phosphatidylinositol synthase; PLA_2, phospholipase A_2; PMT, phos-pho-ethanolamine N-methyltransferase; PS, phosphatidylserine; PSD, PS decarboxylase; PSS, PS synthase; PV, parasitophorous vacuole; Ser, serine; SM, sphingomyelin

synthesis and lipolysis (reviewed in Wilson & Knoll, 2018). Noteworthy, PNPLAs can also be found in prokaryotic microbes like *Legionella pneumophila*. *Legionella* injects the virulence factor VipD, which has PLA activity, into the host cell, where it localizes to early endosome membranes (Gaspar & Machner, 2014; Ku et al., 2012; Shohdy, Efe, Emr, & Shuman, 2005; Zhu, Hammad, Hsu, Mao, & Luo, 2013). Dependent on its PLA_1 activity, it alters associated lipids and proteins and thereby avoids endosomal fusion. Another report described that PLA_2-acting VipD hydrolyses PC and PE of the mitochondrial membrane, which leads to the formation of reactive lysophospholipids (Zhu et al., 2013). These, in consequence, help to destabilize the mitochondrial membrane, resulting in the programmed killing of the infected host cell.

In view of our data, we postulate that the higher PC levels due to PNPLA1-deficiency prevent malaria parasites from entering the sexual pathway. PC biosynthesis is mandatory for the parasite to maintain intraerythrocytic replication, while, due to the activation of the PMT pathway, gametocytes may be able to better synthesize PC under reduced levels of PC precursors in the serum. Future studies need to identify how the malaria parasite monitors its phospholipid levels and unveil the downstream signalling pathways leading to the activation of transcriptional regulators of sexual commitment.

4 | EXPERIMENTAL PROCEDURES

4.1 | Gene identifiers

The following PlasmoDB gene identification numbers are assigned to the genes and proteins investigated in this study: ActinI (PlasmoDB: PF3D7_1246200); Aldolase (PlasmoDB: PF3D7_1444800); alpha/beta hydrolase (PlasmoDB: PF3D7_1001600); AMA1 (PlasmoDB: PF3D7_1133400); AP2-G (PlasmoDB: PF3D7_1222600); ApiAP2 (PlasmoDB: PF3D7_0516800); CRT (PF3D7_0709000); EK (PlasmoDB: PF3D7_1124600); Falcilysin (PlasmoDB: PF3D7_1360800); FNPA (PlasmoDB: PF3D7_1451600); GAPDH (PF3D7_1462800); GDV1 (PlasmoDB: PF3D7_0935400); *Pf*39 (PlasmoDB: PF3D7_1108600); *Pf*CCp2 (PlasmoDB:

PF3D7_1455800); *Pf*s230 (PlasmoDB: PF3D7_0209000); *Pf*s25 (PlasmoDB: PF3D7_1031000); PMT (PlasmoDB: PF3D7_1343000); PNPLA1 (PlasmoDB: Pf3D7_0209100); REX1 (PF3D7_0935900); SAMS (PlasmoDB: PF3D7_0922200); SBP1 (PF3D7_0501300); serine tRNA-ligase (PlasmoDB: PF3D7_0717700); Sir2A (PlasmoDB: PF3D7_1328800).

4.2 | Primary antibodies

In this study, the following primary antibodies and antisera were used: Rabbit anti-HA antibody (Sigma-Aldrich); rat anti-HA antibody (Roche); mouse anti-GFP antibody (Sigma-Aldrich); rabbit polyclonal antisera against *Pf*s230 (Biogenes), *Pf*s25 (ATCC), *Pf*s16 (Lanfrancotti, Bertuccini, Silvestrini, & Alano, 2007), AMA1 (Boes et al., 2015); mouse polyclonal antisera against falcilysin (Weißbach et al., 2017), *Pf*39 (Simon et al., 2009) and actin I (Ngwa et al., 2013). The generation of polyclonal mouse antisera against PNPLA1rp1 and PNPLA1rp2 is described below.

4.3 | Bioinformatics

For 3D modelling of PNPLA1, the I-Tasser server was used (http://zhanglab.ccmb.med.umich.edu/I-TASSER/; Yang et al., 2015). The 3D model was visualised using the iCn3D macromolecular structure viewer (Wang, Geer, Chappey, Kans, & Bryant, 2000). For sequence alignment of homologous proteins, the Clone Manager 9 software was used. The generation of the phylogenetic tree was done with Molecular Evolutionary Genetics Analysis software version 7.0 (Kumar, Stecher, & Tamura, 2016).

4.4 | Parasite culture

Gametocyte producing strain *P. falciparum* NF54 was cultivated *in vitro* in RPMI 1640/HEPES medium (Gibco) supplemented with 10% v/v heat-inactivated human serum (HIS) and A^+ erythrocytes at a 2% v/v hematocrit as described (Ifediba & Vanderberg, 1981; Trager & Jensen, 1976). Medium was completed with 50 μg/ml hypoxanthine (Sigma Aldrich) and 10 μg/ml gentamicin (Gibco) and cultures were grown in an atmosphere of 5% CO_2, 5% O_2 and 90% N_2 at a constant temperature of 37°C. For cultivation of PNPLA1-KO parasites, the selection drug blasticidin (InvivoGen) was added in a final concentration of 5.4 μM; for cultivation of the PNPLA1-KD, the *crt/fnpa*-PNPLA1-GFP/WT and the *crt/fnpa*-PNPLA1-GFP/C11 lines the selection drug WR99210 (Jacobus Pharmaceutical Company) was added in a final concentration of 2.5 nM. Human serum and erythrocyte concentrate were obtained from the Department of Transfusion Medicine, University Hospital Aachen, Germany. Donor sera and blood samples were pooled and kept anonymous. The work with human blood was approved by the Ethics commission of the RWTH University Hospital. The serum-free medium -SerM was prepared as described previously by replacing HIS with oleic and palmitic acid (Sigma Aldrich) in a final concentration of 30 μM each, sodium bicarbonate (Sigma Aldrich) in a final concentration of 24 mM and fatty acid-free BSA (Sigma Aldrich) in a final concentration of 0.39% m/v (Brancucci et al., 2017). The -SerM+lysoPC medium was prepared by adding lysoPC (Avanti Polar Lipids) to -SerM medium in a final concentration of 20 μM; -SerM+Choline medium was prepared by adding choline (Sigma Aldrich) to -SerM medium in a final concentration of 300 μM and glucose in a final concentration of 11.1 mM (Brancucci et al., 2017). The -SerM+Serum medium was prepared by adding 10% HIS to -SerM. To synchronize the asexual parasite blood stages, parasites cultures with 3–4% ring stages were centrifuged, the pellet was resuspended in five times pellet's volume of 5% sorbitol (AppliChem)/ddH20 and incubated for 10 min at room temperature (RT; Lambros & Vanderberg, 1979). Cells were washed once with RPMI to remove sorbitol and further cultivated as described above. To tightly synchronize cultures to a 4-hr time window, consecutive sorbitol treatments were applied as described (Brancucci et al., 2017; Brancucci, Goldowitz, Buchholz, Werling, & Marti, 2015). Mature schizonts and gametocytes were enriched via Percoll gradient centrifugation (GE Healthcare Life Sciences) as described previously (Kariuki et al., 1998; Radfar et al., 2009). Gametogenesis was induced *in vitro* by incubating mature gametocyte cultures in 100 μM xanthurenic acid (XA) dissolved in 1% v/v 0.5 M NH_4OH/ddH_20 for 15 min at RT (Billker et al., 1998; Garcia, Wirtz, Barr, Woolfitt, & Rosenberg, 1998).

4.5 | Recombinant protein expression

Recombinant proteins corresponding to PNPLA1rp1 (spanning aa 498–670) and PNPLA1rp2 (spanning aa 335–496) were expressed as fusion proteins with an N-terminal maltose binding protein (MBP)-tag using the pMAL^{TM}c5x-vector (New England Biolabs). Cloning was mediated by the addition of the restriction sites XmnI/PstI to the ends of gene fragments PCR-amplified from *P. falciparum* gDNA, using PNPLA1rp1 forward primer and PNPLA1rp1 reverse primer for PNPLA1rp1 and PNPLA1 rp2 forward primer and PNPLA1 rp2 reverse primer for PNPLA1rp2 (for primer sequences, see Table S1). Recombinant proteins were expressed using *E. coli* BL21 (DE3) RIL according to the manufacturer's protocol (Stratagene). The recombinant fusion proteins were purified via affinity chromatography from bacterial extracts using amylose resin (New England Biolabs) according to manufacturer's protocol. The full-length recombinant protein corresponding to PNPLA1rp3 (spanning aa 001–679) was expressed as fusion protein with an N-terminal glutathione-S-transferase (GST)-tag using the pGEX-6P-1 vector (GE Healthcare). A synthetic PNPLA1 gene, codon-optimised for recombinant protein expression in *E. coli* with the GeneOptimizerTM software (Thermo Fisher Scientific), was used as template DNA (for synthetic sequence, see Figure S18). Cloning was mediated by the addition of the restriction sites

BamHI and XhoI to the ends of gene fragments PCR-amplified from codon-optimised DNA-template using the PNPLA1rp3 forward primer and PNPLA1rp3 reverse primer (for primer sequences, see Table S1). Recombinant proteins were expressed using *E.coli* BL21 (DE3) RIL according to the manufacturer's protocol.

4.6 | Generation of mouse antisera

Recombinant fusion proteins PNPLA1rp1-MBP and PNPLA1rp2-MBP were purified via affinity chromatography as described above followed by PBS buffer exchange via filter centrifugation using Amicon Ultra 15 (Sigma-Aldrich) according to the manufacturer's protocol. Protein concentrations were determined via Bradford assay. Immune sera were generated by immunisation of 6 weeks old female NMRI mice (Charles Liver Laboratories) via subcutaneous injection of 100 μg recombinant protein emulsified in Freund's incomplete adjuvant (Sigma-Aldrich) followed by a boost after 4 weeks with 50 μg of recombinant protein. Mice were anaesthetised 10 days after the boost by intraperitoneal injection of ketamine–xylazine mixture according to the manufacturer's protocol (Sigma-Aldrich). Polyclonal immune sera were collected via heart puncture and pooled from three mice immunised with the same antigen. NMS were collected for negative control in the experiments. Experiments for the generation of antisera in mice were approved by the animal welfare committees of the District Council of Cologne, Germany (ref. no. 84-02.05.30.12.097 TVA).

4.7 | Generation of the PNPLA1-KO parasite lines

PNPLA1-KO parasite lines were generated via single cross-over homologous recombination using the pCAM-BSD-KO vector (Bennink et al., 2018; Dorin-Semblat et al., 2007; Wirth et al., 2014; Wirth, Bennink, Scheuermayer, Fischer, & Pradel,). A 567 bp gene fragment homologous to the PNPLA1 gene coding for the N-terminal part was amplified via PCR using the PNPLA1-KO forward and reverse primers (for primer sequences, see Table S1). Ligation of insert and vector backbone was mediated by BamHI/NotI restriction sites. A WT culture synchronised for 5% ring stages was loaded with 100 μg vector in transfection buffer via electroporation (310 V, 950 μF, 10 ms; Bio-Rad gene-pulser) as described (Ngwa et al., 2017; Wirth et al., 2014). Blasticidin (InvivoGen) was added to a final concentration of 5.4 μM at 6 hr post-transfection. A mock control was electroporated using transfection buffer only without addition of vector-DNA und cultured in regular A +-medium. Blasticidin-resistant parasites appeared after 3–4 weeks. To confirm successful plasmid integration into the *pnpla1* gene locus, genomic DNA (gDNA) of transfected parasites was isolated using the NucleoSpin Blood Kit (MACHEREY-NAGEL) according to the manufacture's protocol and used as template in diagnostic PCR. The following primers were used to confirm correct integration of the vector into the target locus: (a) PNPLA1-KO 5′-integration forward primer, (b) PNPLA1-KO 3′-integration reverse primer, (c) pCAM-BSD forward primer and (d) pCAM-BSD reverse primer (for primer location, see Figure S5a; for primer sequences, see Table S1). Successful confirmation of vector integration was followed by clonal dilution of a >3% ring stage culture in a 96-well plate. After three weeks of cultivation, clonal subcultures were identified via Malstat assay as described below and subsequent diagnostic PCR was performed to confirm correct integration and absence of the WT *pnpla1* gene locus. Two clonal lines, PNPLA1-KO A12 and PNPLA1-KO C11, were isolated.

4.8 | Generation of the PNPLA1-KD parasite line

PNPLA1-KD parasite lines were generated via single cross-over homologous recombination using the pARL-HA-*glmS* vector (Figure S3). An 867-bp gene fragment homologous to the PNPLA1 gene coding for the C-terminal part was amplified using the PNPLA1-KD forward primer and the PLPLA1-KD reverse primer (for primer sequences, see Table S1). The stop codon was excluded from the homologous gene fragment. Ligation of the insert with the vector backbone was mediated by NotI and AvrII restriction sites. Transfection of parasites was performed as described above. For selection of parasites carrying the vector, WR92210 (Jacobus Pharmaceutical Company) was added to a final concentration of 2.5 nM and successful integration of the vector was confirmed by diagnostic integration PCR using (a) PNPLA1-KD 5'-integration primer, (b) PNPLA1-KD 3′-integration primer, (c) pARL-HA-*glmS* forward primer and (d) pARL-HA-*glmS* reverse primer (for primer location, see Figure S7a; for primer sequences, see Table S1).

4.9 | Generation of the PNPLA1-GFP episomal expression parasite lines

The *crt/fnpa*-PNPLA1-GFP/WT and the *crt/fnpa*-PNPLA1-GFP/C11 parasite lines were generated using the pARLII-GFP vector (Figure S10a). The *pnpla1* full-length gene was amplified from cDNA using the PNPLA1-gfp forward primer and the PNPLA1-gfp reverse primer (for primer location, see Figure S13a; for primer sequences, see Table S1). The stop codon was excluded from the full-length gene sequence. Ligation of the insert with the vector backbones was mediated by XhoI and AvrII. The plasmid was sequenced to confirm that the encoding segment was inserted in frame with the GFP-encoding sequence. Transfection of parasites was performed as described above. For selection of parasites carrying the vectors, WR92210 (Jacobus Pharmaceutical Company) was added to a final concentration of 2.5 nM and successful uptake of the vector was confirmed by diagnostic PCR using the PNPLA1-gfp episome forward primer and the PNPLA1-gfp episome reverse primer (for primer location, see Figure S13; for primer sequences, see Table S1).

4.10 | Indirect immunofluorescence assay and life cell imaging

Mixed asexual blood stage and gametocyte cultures as well as macrogametes collected at 15 or 30 min p.a., of the WT, the PNPLA1-KD and the PNPLA1-KO lines A12 and C11 were air-dried as cell monolayers on glass slides and subsequently fixed with 4% w/v paraformaldehyde/PBS (pH 7.4) for 10 min at RT. For membrane permeabilisation, the fixed parasites were incubated with 0.1% v/v Triton X 100/125 mM glycerine for 10 min, followed by blocking of non-specific binding sites using 3% w/v BSA/PBS for 30 min at RT. For methanol fixation, air-dried cell monolayers were fixed in a methanol bath at −80°C for 10 min. For membrane permeabilisation and blocking of non-specific binding, fixed cells were sequentially incubated in 0.01% w/v saponin/0.5 % w/v BSA/PBS and 1% v/v neutral goat serum (Sigma-Aldrich)/PBS for 30 min at RT. After blocking, the preparations were incubated with polyclonal mouse antisera specific for PNPLA1rp1 and PNPLA1rp2 (dilution 1:200), rabbit anti-HA antiserum (dilution 1:200), rat anti-HA antibody (dilution 1:200) or NMS (dilution 1:200), diluted in 0.5% w/v BSA/PBS for 2 hr at 37°C. Binding of the primary antibody was detected by incubation with Alexa Fluor 488-conjugated goat anti-mouse or secondary antibody (Invitrogen Molecular Probes). The sexual stages were highlighted by double-labelling with rabbit antibodies directed against *Pfs*230, followed by incubation with polyclonal Alexa Fluor 594-conjugated goat anti-rabbit secondary antibodies (Invitrogen Molecular Probes), while the asexual blood stages were stained with 0.001% w/v Evans Blue (EB) (Sigma Aldrich)/PBS for 3 min at RT followed by 5 min washing with PBS. The parasite nuclei were highlighted by treatment with Hoechst 33342 nuclear stain (Invitrogen) for 1 min at RT. Cells were washed with PBS and mounted with anti-fading solution AF2 (CitiFluor™) and sealed with nail polish. Specimens were examined with a Leica DM 5500 B microscope and digital images were processed using the Adobe Photoshop CS software. For life cell imaging, mixed asexual blood stages or gametocyte of the PNPLA1-GFP expressing *crt/fnpa*-PNPLA1-GFP/WT lines were seeded as cell monolayers on glass slides and imaged on a Leica DM 5500 B microscope. Digital images were processed using the Adobe Photoshop CS software. For visualisation of the parasites' nuclei DNA, 1 μg/ml Hoechst33342 was added to the specimen before image acquisition.

4.11 | Merozoite quantification

Cell monolayers of synchronised mature schizonts of WT and of PNPLA-KO A12 and PNPLA1-KO C11 were air-dried on glass slides and subsequently fixed with 4% w/v paraformaldehyde/PBS (pH 7.4) for 10 min. Counterstaining with EB and highlighting of nuclei by Hoechst 33342 nuclear stain was performed as described above. Specimens were examined with a Leica DM 5500 B microscope and number of nuclei of mononucleated merozoites was counted for 75 schizonts per setting. Only mature schizonts that had clearly segmented merozoites with limited overlap and with single pigmented residual bodies indicating singular infections were used for the analysis.

4.12 | Diagnostic RT-PCR

Total RNA was isolated from sorbitol-synchronised ring, trophozoite and schizont cultures, as well as from Percoll-gradient enriched immature (Stage II–IV), mature (Stage V) and activated gametocytes (15 min p.a.) of the WT using the Trizol reagent (Invitrogen) according to the manufacture's protocol. RNA was prepared by phenol/chloroform preparations followed by ethanol precipitation and subsequent treatment with RNase-free DNase I (Qiagen). Photometric analyses of RNA samples all had A260/280 ratios higher than 2.1. Two micrograms of each RNA sample were used as template for cDNA synthesis using the SuperscriptIV First-Strand Synthesis System (Invitrogen) according to manufacturer's protocol. Transcript for PNPLA1 (220 bp) was amplified in 25 cycles using PNPLA1 RT forward and reverse primers (for primer sequences, see Table S1). To confirm the purity of the asexual blood stage and gametocyte samples, transcript amplifications of *ama1* (407 bp) using AMA1-RT forward and reverse primers and of *ccp2* (286 bp) using CCP2-RT forward and reverse primers were performed (Peterson et al., 1989; Pradel et al., 2004). To confirm synchronisation of the ring stages used for the lipidomics analysis, cDNA has been prepared from a small proportion of corresponding cultures as described and transcript amplifications of the ring stage-specific gene *rex1* (342 bp) using REX1-RT forward and reverse primers and of *ccp2* (286 bp, negative control) using CCP2-RT forward and reverse primers were performed. Amplification of the housekeeping gene *aldolase* (378 bp) was used as loading control and to test for residual genomic DNA in the negative controls without reverse transcriptase. PCR products were separated by 1.5% agarose gel electrophoresis.

4.13 | Real-time RT-PCR

RNA from asexual blood stages, including synchronised ring stages used for the lipidomics analyses, was isolated as described above and 2 μg of each total RNA sample was used as template for cDNA synthesis using the Super Script IV First-Strand Synthesis System (Invitrogen) following the manufacturer's protocol. The synthesised cDNA was first tested by diagnostic RT-PCR for purity of the asexual blood stages or synchronised ring stages, using either *ama1*-, *ccp2*- or *rex1*-specific primers, respectively. Controls without reverse transcriptase were used to exclude potential genomic DNA contamination by using *aldolase* primers. All primers used for real-time RT-PCR are listed in Table S1. The primers were designed using the Primer 3 software (Primer3 Input; version 0.4.0) and were initially tested for specificity via conventional PCR on gDNA. Real-time RT-PCR measurements were performed using the StepOnePlus Real-Time PCR System (Applied Biosystems). Samples were analysed in triplicate in a total

volume of 20 μl using the maxima SYBR green qPCR master mix according to manufacturer's instructions (Thermo Scientific). Controls without template and without reverse transcriptase were included in all real-time RT-PCR experiments. Transcript expression levels were calculated by the $2^{-\Delta\Delta Ct}$ (Livak & Schmittgen, 2001) method using the endogenous control gene encoding the *P. falciparum* seryl tRNA-ligase (PF3D7_0717700) as reference (Bennink et al., 2018; Ngwa et al., 2017; Salanti et al., 2003).

4.14 | Subcellular fractioning

The protocol for subcellular fractionation of parasite lysates using the solubility of proteins in different buffers was modified from Grüring et al. (2012). In brief, ~3 × 10^6 schizonts of the PNPLA1-KD line were purified via Percoll gradient and liberated from the RBCs with 0.03% saponin/PBS for 3 min at 4°C. After washing with PBS, parasites were hypotonically lysed in 100 μl of 5 mM Tris-HCL (pH 8), supplemented with protease inhibitor cocktail (complete EDTA-free, Roche) for 10 min at RT followed by freezing at −20°C and thawing on ice. Soluble proteins (Tris-HCl fraction) were separated from non-soluble constituents by centrifugation (5 min, 16,000*g*, 4°C). This was followed by sequential pellet extraction with 100 μl each of freshly prepared Na_2CO_3 on ice for 30 min (peripheral fraction), ice-cold 1% Triton X-100 (integral membrane fraction) and 0.5× PBS/4% SDS/0.5% Triton X-100 (insoluble fraction) at RT. Between each extraction, the remaining pellet was washed with 1 ml ice-cold PBS to remove any impurities. Supernatants were centrifuged to remove residual material. The individual fractions were subjected to WB as described below.

4.15 | Western blotting

Asexual blood stage parasites of the WT, the PNPLA1-KO lines A12 and C11, the PNPLA1-KD line and the *crt/fnpa*-PNPLA1-GFP/C11 lines were harvested from mixed or synchronised cultures, while gametocytes were enriched by Percoll purification. Parasites were released from iRBCs with 0.015% w/v saponin/PBS for 10 min at 4°C, washed with PBS and resuspended in lysis buffer (0.5% Triton X-100, 4% w/v SDS, 0.5× PBS) supplemented with protease inhibitor cocktail (Roche). 5×SDS-PAGE loading buffer containing 25 mM dithiothreitol was added to the lysates, samples were heat-denatured for 10 min at 95°C and separated via SDS-PAGE. Following gel electrophoresis, separated parasite proteins were transferred to Hybond ECL nitrocellulose membrane (Amersham Biosciences) according to the manufacturer's protocol. Non-specific binding was blocked by incubation of the membranes in Tris-buffered saline containing 5% w/v skim milk, pH 7.5, followed by immune recognition overnight at 4°C using polyclonal mouse immune sera specific for *Pf*39 (dilution 1:5,000), PfAMA1 (dilution 1:1,000), falcilysin (1:1,000), actin I (1:1,000), PNPLA1rp1 (1:1,000), PNPLA1rp2 (1:1,000), mouse anti-GFP antibody (1:1,000) or using polyclonal rabbit immune sera specific to anti-HA (1:1,000). After washing, membranes were incubated with the respective alkaline phosphatase-conjugated secondary antibody (Sigma-Aldrich) for 1 hr at RT and developed in a solution of nitroblue tetrazolium chloride (NBT) and 5-bromo-4-chloro-3-indoxylphosphate (BCIP; Sigma-Aldrich) for 5–30 min at RT. Blots were scanned and processed using the Adobe Photoshop CS software. Band intensities were measured using the ImageJ programme version 1.51f.

4.16 | Asexual blood stage replication assay

4.16.1 | PNPLA1-KO lines

To compare asexual blood stage replication between the parental WT and the PNPLA1-KO lines A12 and C11, synchronised asexual blood stage cultures were set to an initial parasitemia of 0.25% ring stages und cultivated as described above. Giemsa-stained thin blood smears were prepared every 24 hr over a time-period of 120 hr at six different time points (0, 24, 48, 72, 96 and 120 hr post-seeding). Parasitemia of each time point was determined microscopically at 1,000-fold magnification by counting the percentage of parasites in 1,000 RBCs. To identify the blood stages (ring, trophozoites, schizonts and mature schizonts) present in the cultures at a given time point, 100 iRBCs were counted per setting.

4.16.2 | PNPLA1-KD line

To analyse asexual blood stage replication and length of the intraerythrocytic replication cycle in the PNPLA1-KD parasite line, experiments were set-up as described above. Expression of PNPLA1 was knocked-down in transgenic PNPLA1-KD parasite line by treatment of the culture with GlcN (D-(+)-glucosamine hydrochloride; Sigma Aldrich) at a final concentration of 2.5 mM. GlcN treatment started one cycle before the experimental set-up. The GlcN-treated culture was compared to the untreated culture cultivated in normal cell culture medium. To exclude an unspecific effect of GlcN, the parental WT line was used as control. For each assay, three experiments were performed, each in triplicate. Data analysis was performed using MS Excel 2014.

4.17 | Gametocyte development assay

4.17.1 | PNPLA1-KO lines

To compare gametocyte development between the WT and the PNPLA1-KO lines A12 and C11, tightly synchronised ring stage

cultures were set to a parasitemia of 2% with 5% hematocrit and cultivated in cell culture medium at 37°C. The medium was exchanged daily. Cultures were maintained in cell culture medium over a time period of 14 days and samples were taken in triplicate every 24 hr starting from day 2 p.g.i. for Giemsa smear preparation. To induce sexual differentiation with -SerM medium, tightly synchronised parasites (28 ± 2 h.p.i.) with a 1% parasitemia at 5% hematocrit were incubated for 22 hr in -SerM as described (Brancucci et al., 2017). Incubation with -SerM was followed by cultivation in cell culture medium supplemented with 50 mM GlcNAc (N-acetyl glucosamine) to kill the asexual blood stages. Samples were taken in triplicate every 24 hr starting from day 2 p.g.i. for Giemsa smear preparation. Cultures cultivated in -SerM+lysoPC, -SerM+Choline and -SerM+Serum were used as control (Brancucci et al., 2017). To test the effect of 4-BPB on gametocyte induction, cultures were set up as described above and the -SerM medium was supplemented with the respective inhibitor at IC_{50} concentration. Cultures treated with -SerM with or without 1% v/v DMSO were used as controls. Gametocytemia was determined per 1,000 RBCs and the gametocyte stages II-IV at the different time points were recorded. For each assay, three experiments were performed, each in triplicate. Data analysis was performed using MS Excel 2014 and GraphPad Prism 5.

4.17.2 | PNPLA1-KD line

To analyse gametocytogenesis in the PNPLA1-KD line, expression of PNPLA1 was knocked-down by supplementation of the cell culture medium with the inducer GlcN at a final concentration of 2.5 mM. GlcN was added one cycle before the experimental set-up. The GlcN-treated culture was compared to the untreated cultures. To exclude an unspecific effect of GlcN, the parental WT was used as control. To compare gametocyte development between the treated and untreated PNPLA1-KD line, tightly synchronised ring stage cultures were set to a parasitemia of 2% with 5% hematocrit and cultivated in cell culture medium at 37°C. The medium was exchanged daily. Cultures were maintained in cell culture medium over a time period of 14 days and samples were taken in triplicate every 24 hr starting from day 2 p.g.i. for Giemsa smear preparation. To determine the effect of PNPLA1-deficiency on gametocytogenesis before or after gametocyte induction, tightly synchronised ring stage parasite cultures were maintained in cell medium until a parasitemia of 10% was reached. Gametocytogenesis was induced by addition of lysed RBCs for 24 hr (Ngwa et al., 2017; Schneweis, Maier, & Seitz, 1991). Cells were washed and cultures were maintained in cell culture medium supplemented with 50 mM GlcNAc for ~5 days to kill the asexual blood stages followed by cultivation in normal cell culture medium (Fivelman et al., 2007; Ngwa et al., 2017). GlcN was either added before addition or after removal of gametocyte-promoting lysed RBCs. To induce sexual differentiation with -SerM medium, tightly synchronised parasites (28 ± 2 h.p.i.) with a 1% parasitemia at 5% hematocrit were incubated for 22 hr in -SerM as described (Brancucci et al., 2017). Incubation with -SerM was followed by cultivation in cell culture medium supplemented with 50 mM GlcNAc to kill the asexual blood stages. Samples were taken in triplicate every 24 hr starting from day 2 p.g.i. for Giemsa smear preparation. Cultures cultivated in -SerM+lysoPC and -SerM+Choline were used as control (Brancucci et al., 2017).

To test the effect of 4-BPB on gametocyte induction, the -SerM medium was supplemented with the respective inhibitor at IC_{50} concentration. Cultures treated with -SerM with or without 1% v/v DMSO were used as controls. Gametocytemia was determined per 1,000 RBCs and the gametocyte stages II–IV at the different time points were recorded. For each assay, three experiments were performed, each in triplicate. Data analysis was performed using MS Excel 2014 and GraphPad Prism 5.

4.17.3 | PNPLA1-GFP overexpression lines

To analyse gametocytogenesis in the *crt/fnpa*-PNPLA1-GFP/WT or *crt/fnpa*-PNPLA1-GFP/C11 lines, tightly synchronised parasites (28 ± 2 h.p.i.) with a 1% parasitemia at 5% hematocrit were incubated for 22 hr in -SerM as described (Brancucci et al., 2017). Incubation with -SerM was followed by cultivation in cell culture medium supplemented with 50 mM GlcNAc to kill the asexual blood stages. Samples were taken in triplicate every 24 hr starting from day 2 p.g.i. for Giemsa smear preparation. Gametocytemia was determined per 1,000 RBCs. For each assay, three independent experiments were performed, each in triplicate. Data analysis was performed using MS Excel 2014 and GraphPad Prism 5.

4.18 | Comparative exflagellation assay

At Day 14 p.g.i., mature gametocytes of the WT and the PNPLA1-KO lines A12 and C11 were adjusted with erythrocytes to a final gametocytemia of 1% with a total hematocrit of 5% in cell culture medium. A volume of 100 µl of each gametocyte culture was activated *in vitro* with 100 µM XA for 15 min at RT. At 15 min p.a., the numbers of exflagellation centres were counted at 400-fold magnification in 30 optical fields using a Leica DMLS microscope. Four independent experiments were conducted in quadruplicate; data analysis was performed using MS Excel 2014. Exflagellation was calculated as a percentage of the number of exflagellation centres in the PNPLA1-KO lines in relation to the number of exflagellation centres in the WT control (WT set to 100%).

4.19 | Comparative macrogamete and zygote formation assay

For the analysis of macrogamete and zygote formation, mature gametocytes of the WT and of the PNPLA1-KO lines A12 and C11 were enriched via Percoll purification and adjusted to a final gametocytemia of 2% with a total hematocrit of 5% in cell culture medium.

Gametocyte cultures were activated *in vitro* with 100 μM XA for 30 min (macrogametes) or 6 hr (zygotes) at RT. An equal volume of each sample was coated on Teflon slides and subjected to IFA as described above using rabbit anti-*Pfs*25 antisera for macrogamete and zygote labelling. Parasites were counted microscopically using a Leica DM 5500B fluorescence microscope with 600-fold magnification. Numbers of macrogametes and zygotes were counted for a total number of 1,000 erythrocytes in triplicate and calculated in relation to the WT control (set to 100%). For each assay, three experiments were performed, each in triplicate. Data analysis was performed using MS Excel 2014.

4.20 | Malstat assay

To determine the antimalarial effect of the phospholipase inhibitors 2,4′-dibromoacetophenone (4-BPB; Sigma Aldrich), ASB14780 (Sigma Aldrich), N-(*p*-amylcinnamoyl) anthranilic acid (Biomol) and bromoenol lactone (Biomol), a Malstat assay was performed as described previously (Aminake et al., 2011). Synchronised ring stages of the WT were plated in triplicate in a 96-well plate (200 μl/well) at a parasitemia of 1.0% in the presence of the respective inhibitor dissolved in DMSO (500 μM to 0.05 nM for 4-BPB and N-(*p*-amylcinnamoyl) anthranilic acid and 1 mM to 7.8 μM for bromoenol lactone and ASB14780). Chloroquine, dissolved in RPMI, served as positive control, DMSO alone at a concentration of 0.5% v/v was used as negative control. Parasites were cultivated *in vitro* in an airtight container as described above. After 72 hr, 20 μl of each well were mixed with 100 μl Malstat reagent in a new 96-well microtiter plate. Parasite lactate dehydrogenase activity was measured by adding 20 μl of a 1:1 mixture of 1 mg/ml diaphorase and 1 mg/ml NBT (nitroblue tetrazolium) to the Malstat reaction, and optical densities were measured at 630 nm. Three experiments were performed, each in triplicate. The IC_{50} values were calculated from variable-slope sigmoidal dose–response curves using the GraphPad Prism 5 program.

4.21 | Gametocyte toxicity assay

WT parasites were grown at high parasitemia to induce gametocyte formation. When stage II gametocytes were formed, 1 ml of the culture was plated in triplicate in 24-well plate and incubated with 4-BPB at IC_{50} (5.6 μM) concentration. Chloroquine at IC_{50} (12 nM) concentration and 0.5% v/v DMSO served as negative controls. The proteasome inhibitor epoxomicin (60 nM) was diluted in DMSO and used as positive control (Aminake et al., 2011; Ngwa et al., 2017). The parasites were treated with inhibitors for 2 days and the medium was replaced daily. The parasites were cultivated for 10 days and Giemsa-stained blood smears were taken at Day 7 and Day 10 to determine numbers of gametocytes of Stages IV and V per 1,000 RBCs. Three experiments were performed, each in triplicate. Data analysis was performed using MS Excel 2014 and GraphPad Prism 5.

4.22 | Lipidomics analysis

Lipidomics analysis was performed on four independent cell harvests of the WT and the PNPLA1-KO lines A12 and C11. Highly synchronous parasite cultures were harvested by transferring the cultures to pre-warmed 50-ml tubes and the total amount of parasites were determined by Giemsa staining and via counting on a haemocytometer. The cultures were metabolically quenched via rapid cooling to 0°C by suspending the tube over a dry ice/100% ethanol slurry mix, while continually stirring the solution. Following quenching, parasites were constantly kept at 4°C and liberated from the enveloping RBCs by mild saponin treatment with 0.15% w/v saponin/0.1% w/v BSA PBS for 5 min. RBC lysis was verified by Giemsa smear and the purity of the synchronised ring stages was confirmed by diagnostic and real-time RT-PCR (see above). After three washing steps with 1 ml ice-cold PBS followed by centrifugation each time, the parasite pellet was subjected to lipid extraction using chloroform and methanol (Amiar et al., 2016) in the presence of butylhydoxytluene, PC (C21:0/C21:0), C13:0 fatty acids and Lipidomix lipid standard mix (Avanti). Then the extract was set to biphase separation with 0.2% KCl to remove polar molecules. The total lipid extract was dried under the nitrogen gas. The lipid was then dissolved in the 1-butanol and separated by two-dimensional high-performance thin layer chromatography (NanoSiL, MACHEREY-NAGEL). For the first dimension, the solvent system of chloroform/methanol/28% ammonium hydroixide (65:35:8, v/v/v) and for the second dimension, chloroform/acetone/methanol/acetic acid/water, 40:15:14:13:7.5 (v/v/v/v/v) were used, respectively. Each lipid spot was confirmed with authentic standards. The lipid spot was then scraped off and set to methanolysis with C15:0 fatty acid standard in 0.5 M HCl/methanol at 85°C for 6 hr. Generated fatty acid methyl esters were then extracted by hexane. Fatty acid methyl esters were detected by GC-MS (Agilent 5977A-7890B) according to the method described in Ramakrishnan et al. (2012) and quantified by Mass Hunter software (Agilent). Each fatty acid was quantified according the calibration curve generated with authentic fatty methyl ester standards.

4.23 | Statistical analysis

Data are expressed as mean ± *SD*. Statistical differences were determined using one-way ANOVA with post hoc Bonferroni multiple comparison test or unpaired tow-tailed Student's *t* test, as indicated. Values of $p < 0.05$ were considered statistically significant. Significances were calculated using GraphPad Prism 5 and are represented in the figures as follows: ns, not significant $p > 0.05$; *$p < 0.05$; **$p < 0.01$; ***$p < 0.001$.

ACKNOWLEDGEMENTS

The authors thank Matthias Marti (University of Glasgow) and Chetan Chitnis (Pasteur Institute Paris) for helpful discussions. The authors further thank Christina Lang (Robert Koch Institute) and Jean-Pierre Musabyimana, Alexandra Golzmann and Sofia Basova (RWTH Aachen

University) for support with the experiments. The work was funded by the priority programme SPP1580 of the Deutsche Forschungsgemeinschaft (GP, AF and JMP).

CONFLICT OF INTEREST

The authors have no conflict of interest to declare.

ORCID

Antje Flieger https://orcid.org/0000-0003-3819-2979
Cyrille Botté https://orcid.org/0000-0002-2245-536X
Gabriele Pradel https://orcid.org/0000-0003-2264-5558

REFERENCES

Alano, P. (2007). *Plasmodium falciparum* gametocytes: Still many secrets of a hidden life. *Molecular Microbiology*, *66*(2), 291–302. https://doi.org/10.1111/j.1365-2958.2007.05904.x

Amiar, S., MacRae, J. I., Callahan, D. L., Dubois, D., van Dooren, G. G., Shears, M. J., … Botté, C. Y. (2016). Apicoplast-localized lysophosphatidic acid precursor assembly is required for bulk phospholipid synthesis in *Toxoplasma gondii* and relies on an algal/plant-like glycerol 3-phosphate acyltransferase. *PLoS Pathogens*, *12*(8), e1005765. https://doi.org/10.1371/journal.ppat.1005765

Aminake, M. N., Schoof, S., Sologub, L., Leubner, M., Kirschner, M., Arndt, H.-D., & Pradel, G. (2011). Thiostrepton and Derivatives Exhibit Antimalarial and Gametocytocidal Activity by Dually Targeting Parasite Proteasome and Apicoplast. *Antimicrobial Agents and Chemotherapy*, *55*(4), 1338–1348. https://doi.org/10.1128/AAC.01096-10

Arpigny, J. L., & Jaeger, K. E. (1999). Bacterial lipolytic enzymes: Classification and properties. *The Biochemical Journal*, *343*, 177–183. https://doi.org/10.1042/bj3430177

Aurrecoechea, C., Brestelli, J., Brunk, B. P., Dommer, J., Fischer, S., Gajria, B., … Wang, H. (2009). PlasmoDB: a functional genomic database for malaria parasites. *Nucleic Acids Research*, *37*(Database), D539–D543. https://doi.org/10.1093/nar/gkn814

Banerji, S., & Flieger, A. (2004). Patatin-like proteins: A new family of lipolytic enzymes present in bacteria? *Microbiology*, *150*(3), 522–525. https://doi.org/10.1099/mic.0.26957-0

Barbour, S. E., & Ramanadham, S. (2017). Analyses of Calcium-Independent Phospholipase A2beta (iPLA2β) in Biological Systems. *Methods in Enzymology*, *583*, 119–141. https://doi.org/10.1016/bs.mie.2016.09.001

Baum, J., Gilberger, T.-W., Frischknecht, F., & Meissner, M. (2008). Host-cell invasion by malaria parasites: Insights from Plasmodium and Toxoplasma. *Trends in Parasitology*, *24*(12), 557–563. https://doi.org/10.1016/j.pt.2008.08.006

Beaumelle, B. D., & Vial, H. J. (1988). Uninfected red cells from malaria-infected blood: Alteration of fatty acid composition involving a serum protein: An in vivo and in vitro study. *Vitro Cellular & Developmental Biology: Journal of the Tissue Culture Association*, *24*(7), 711–718. https://doi.org/10.1007/BF02623610

Ben Mamoun, C., Prigge, S. T., & Vial, H. (2010). Targeting the Lipid Metabolic Pathways for the Treatment of Malaria. *Drug Development Research*, *71*(1), 44–55. https://doi.org/10.1002/ddr.20347

Bennink, S., Kiesow, M. J., & Pradel, G. (2016). The development of malaria parasites in the mosquito midgut. *Cellular Microbiology*, *18*(7), 905–918. https://doi.org/10.1111/cmi.12604

Bennink, S., von Bohl, A., Ngwa, C. J., Henschel, L., Kuehn, A., Pilch, N., … Pradel, G. (2018). A seven-helix protein constitutes stress granules crucial for regulating translation during human-to-mosquito transmission of *Plasmodium falciparum*. *PLoS Pathogens*, *14*(8), e1007249. https://doi.org/10.1371/journal.ppat.1007249

Billker, O., Lindo, V., Panico, M., Etienne, A. E., Paxton, T., Dell, A., … Morris, H. R. (1998). Identification of xanthurenic acid as the putative inducer of malaria development in the mosquito. *Nature*, *392*(6673), 289–292. https://doi.org/10.1038/32667

Blisnick, T., Morales Betoulle, M. E., Barale, J.-C., Uzureau, P., Berry, L., Desroses, S., … Braun Breton, C. (2000). Pfsbp1, a Maurer's cleft *Plasmodium falciparum* protein, is associated with the erythrocyte skeleton. *Molecular and Biochemical Parasitology*, *111*(1), 107–121. https://doi.org/10.1016/S0166-6851(00)00301-7

Bobenchik, A. M., Choi, J.-Y., Mishra, A., Rujan, I. N., Hao, B., Voelker, D. R., … Ben Mamoun, C. (2010). Identification of inhibitors of *Plasmodium falciparum* phos-pho-ethanolamine methyltransferase using an enzyme-coupled transmethylation assay. *BMC Biochemistry*, *11*(1), 4. https://doi.org/10.1186/1471-2091-11-4

Boes, A., Spiegel, H., Edgue, G., Kapelski, S., Scheuermayer, M., Fendel, R., … Fischer, R. (2015). Detailed functional characterization of glycosylated and nonglycosylated variants of malaria vaccine candidate PfAMA1 produced in Nicotiana benthamiana and analysis of growth inhibitory responses in rabbits. *Plant Biotechnology Journal*, *13*(2), 222–234. https://doi.org/10.1111/pbi.12255

Botté, C. Y., Yamaryo-Botté, Y., Rupasinghe, T. W. T., Mullin, K. A., MacRae, J. I., Spurck, T. P., … McFadden, G. I. (2013). Atypical lipid composition in the purified relict plastid (apicoplast) of malaria parasites. *Proceedings of the National Academy of Sciences*, *110*(18), 7506–7511. https://doi.org/10.1073/pnas.1301251110

Brancucci, N. M. B., Bertschi, N. L., Zhu, L., Niederwieser, I., Chin, W. H., Wampfler, R., … Voss, T. S. (2014). Heterochromatin Protein 1 Secures Survival and Transmission of Malaria Parasites. *Cell Host & Microbe*, *16*(2), 165–176. https://doi.org/10.1016/j.chom.2014.07.004

Brancucci, N. M. B., De Niz, M., Straub, T. J., Ravel, D., Sollelis, L., Birren, B. W., … Marti, M. (2018). Probing *Plasmodium falciparum* sexual commitment at the single-cell level. *Wellcome Open Research*, *3*, 70. https://doi.org/10.12688/wellcomeopenres.14645.1

Brancucci, N. M. B., Gerdt, J. P., Wang, C., Jiang, H. Y., Clardy, J., Marti, M., … Jiang, R. H. Y. (2017). Lysophosphatidylcholine regulates sexual stage differentiation in the human malaria parasite *Plasmodium falciparum*. *Cell*, *171*(7), 1532–1539. https://doi.org/10.1016/j.cell.2017.10.020

Brancucci, N. M. B., Goldowitz, I., Buchholz, K., Werling, K., & Marti, M. (2015). An assay to probe *Plasmodium falciparum* growth, transmission stage formation and early gametocyte development. *Nature Protocols*, *10*(8), 1131–1142. https://doi.org/10.1038/nprot.2015.072

Cassaing, S., Fauvel, J., Bessières, M.-H., Guy, S., Séguéla, J.-P., & Chap, H. (2000). Toxoplasma gondii secretes a calcium-independent phospholipase A2. *International Journal for Parasitology*, *30*(11), 1137–1142. https://doi.org/10.1016/S0020-7519(00)00101-6

Coleman, B. I., Skillman, K. M., Jiang, R. H. Y., Childs, L. M., Altenhofen, L. M., Ganter, M., … Duraisingh, M. T. (2014). A *Plasmodium falciparum* Histone Deacetylase Regulates Antigenic Variation and Gametocyte Conversion. *Cell Host & Microbe*, *16*(2), 177–186. https://doi.org/10.1016/j.chom.2014.06.014

Cowman, A. F., Healer, J., Marapana, D., & Marsh, K. (2016). Malaria: Biology and Disease. *Cell*, *167*(3), 610–624. https://doi.org/10.1016/j.cell.2016.07.055

Czesny, B., Goshu, S., Cook, J. L., & Williamson, K. C. (2009). The proteasome inhibitor epoxomicin has potent *Plasmodium falciparum* gametocytocidal activity. *Antimicrobial Agents and Chemotherapy*, *53*(10), 4080–4085. https://doi.org/10.1128/AAC.00088-09

Déchamps, S., Maynadier, M., Wein, S., Gannoun-Zaki, L., Maréchal, E., & Vial, H. J. (2010). Rodent and nonrodent malaria parasites differ in their phospholipid metabolic pathways. *Journal of Lipid Research*, *51*(1), 81–96. https://doi.org/10.1194/jlr.M900166-JLR200

Déchamps, S., Shastri, S., Wengelnik, K., & Vial, H. J. (2010). Glycerophospholipid acquisition in Plasmodium—A puzzling assembly

of biosynthetic pathways. *International Journal for Parasitology*, *40*(12), 1347–1365. https://doi.org/10.1016/j.ijpara.2010.05.008

Dhondt, S., Geoffroy, P., Stelmach, B. A., Legrand, M., & Heitz, T. (2000). Soluble phospholipase A2 activity is induced before oxylipin accumulation in tobacco mosaic virus-infected tobacco leaves and is contributed by patatin-like enzymes. *The Plant Journal*, *23*(4), 431–440. https://doi.org/10.1046/j.1365-313x.2000.00802.x

Dhondt, S., Gouzerh, G., Muller, A., Legrand, M., & Heitz, T. (2002). Spatio-temporal expression of patatin-like lipid acyl hydrolases and accumulation of jasmonates in elicitor-treated tobacco leaves are not affected by endogenous levels of salicylic acid. *The Plant Journal*, *32*(5), 749–762. https://doi.org/10.1046/j.1365-313X.2002.01465.x

Dorin-Semblat, D., Quashie, N., Halbert, J., Sicard, A., Doerig, C., Peat, E., … Doerig, C. (2007). Functional characterization of both MAP kinases of the human malaria parasite *Plasmodium falciparum* by reverse genetics. *Molecular Microbiology*, *65*(5), 1170–1180. https://doi.org/10.1111/j.1365-2958.2007.05859.x

Eksi, S., Morahan, B. J., Haile, Y., Furuya, T., Jiang, H., Ali, O., … Williamson, K. C. (2012). *Plasmodium falciparum* gametocyte development 1 (Pfgdv1) and gametocytogenesis early gene identification and commitment to sexual development. *PLoS Pathogens*, *8*(10), e1002964. https://doi.org/10.1371/journal.ppat.1002964

Filarsky, M., Fraschka, S. A., Niederwieser, I., Brancucci, N. M. B., Carrington, E., Carrió, E., … Voss, T. S. (2018). GDV1 induces sexual commitment of malaria parasites by antagonizing HP1-dependent gene silencing. *Science*, *359*(6381), 1259–1263. https://doi.org/10.1126/science.aan6042

Fivelman, Q. L., McRobert, L., Sharp, S., Taylor, C. J., Saeed, M., Swales, C. A., … Baker, D. A. (2007). Improved synchronous production of *Plasmodium falciparum* gametocytes in vitro. *Molecular and Biochemical Parasitology*, *154*(1), 119–123. https://doi.org/10.1016/J.MOLBIOPARA.2007.04.008

Flammersfeld, A., Lang, C., Flieger, A., & Pradel, G. (2018). Phospholipases during membrane dynamics in malaria parasites. *International Journal of Medical Microbiology*, *308*(1), 129–141. https://doi.org/10.1016/j.ijmm.2017.09.015

Garcia, G. E., Wirtz, R. A., Barr, J. R., Woolfitt, A., & Rosenberg, R. (1998). Xanthurenic acid induces gametogenesis in Plasmodium, the malaria parasite. *The Journal of Biological Chemistry*, *273*(20), 12003–12005. https://doi.org/10.1074/JBC.273.20.12003

Gaspar, A. H., & Machner, M. P. (2014). VipD is a Rab5-activated phospholipase A1 that protects Legionella pneumophila from endosomal fusion. *Proceedings of the National Academy of Sciences of the United States of America*, *111*(12), 4560–4565. https://doi.org/10.1073/pnas.1316376111

Grüring, C., Heiber, A., Kruse, F., Flemming, S., Franci, G., Colombo, S. F., … Spielmann, T. (2012). Uncovering common principles in protein export of malaria parasites. *Cell Host & Microbe*, *12*(5), 717–729. https://doi.org/10.1016/J.CHOM.2012.09.010

Gulati, S., Ekland, E. H., Ruggles, K. V., Chan, R. B., Jayabalasingham, B., Zhou, B., … Fidock, D. A. (2015). Profiling the essential nature of lipid metabolism in asexual blood and gametocyte stages of *Plasmodium falciparum*. *Cell Host & Microbe*, *18*(3), 371–381. https://doi.org/10.1016/j.chom.2015.08.003

Haldar, K., & Mohandas, N. (2009). Malaria, erythrocytic infection, and anemia. *Hematology. American Society of Hematology. Education Program*, *10*, 87–93. https://doi.org/10.1182/asheducation-2009.1.87

Hawthorne, P. L., Trenholme, K. R., Skinner-Adams, T. S., Spielmann, T., Fischer, K., Dixon, M. W. A., … Gardiner, D. L. (2004). A novel *Plasmodium falciparum* ring stage protein, REX, is located in Maurer's clefts. *Molecular and Biochemical Parasitology*, *136*(2), 181–189. https://doi.org/10.1016/j.molbiopara.2004.03.013

Ifediba, T., & Vanderberg, J. P. (1981). Complete in vitro maturation of *Plasmodium falciparum* gametocytes. *Nature*, *294*(5839), 364–366. https://doi.org/10.1038/294364a0

Josling, G. A., Williamson, K. C., & Llinás, M. (2018). Regulation of sexual commitment and gametocytogenesis in malaria parasites. *Annual Review of Microbiology*, *72*(1), 501–519. https://doi.org/10.1146/annurev-micro-090817-062712

Kafsack, B. F. C., Rovira-Graells, N., Clark, T. G., Bancells, C., Crowley, V. M., Campino, S. G., … Llinás, M. (2014). A transcriptional switch underlies commitment to sexual development in malaria parasites. *Nature*, *507*(7491), 248–252. https://doi.org/10.1038/nature12920

Kariuki, M. M., Kiaira, J. K., Mulaa, F. K., Mwangi, J. K., Wasunna, M. K., & Martin, S. K. (1998). *Plasmodium falciparum*: Purification of the various gametocyte developmental stages from in vitro-cultivated parasites. *The American Journal of Tropical Medicine and Hygiene*, *59*(4), 505–508. https://doi.org/10.4269/ajtmh.1998.59.505

Kienesberger, P. C., Oberer, M., Lass, A., & Zechner, R. (2009). Mammalian patatin domain containing proteins: A family with diverse lipolytic activities involved in multiple biological functions. *Journal of Lipid Research*, *50*, 63–68. https://doi.org/10.1194/jlr.R800082-JLR200

Ku, B., Lee, K.-H., Park, W. S., Yang, C.-S., Ge, J., Lee, S.-G., … Oh, B.-H. (2012). VipD of Legionella pneumophila Targets Activated Rab5 and Rab22 to Interfere with Endosomal Trafficking in Macrophages. *PLoS Pathogens*, *8*(12), e1003082. https://doi.org/10.1371/journal.ppat.1003082

Kuehn, A., & Pradel, G. (2010). The Coming-Out of Malaria Gametocytes. *Journal of Biomedicine and Biotechnology*, *2010*, 1–11. https://doi.org/10.1155/2010/976827

Külzer, S., Rug, M., Brinkmann, K., Cannon, P., Cowman, A., Lingelbach, K., … Przyborski, J. M. (2010). Parasite-encoded Hsp40 proteins define novel mobile structures in the cytosol of the *P. falciparum*-infected erythrocyte. *Cellular Microbiology*, *12*(10), 1398–1420. https://doi.org/10.1111/j.1462-5822.2010.01477.x

Kumar, S., Stecher, G., & Tamura, K. (2016). MEGA7: Molecular evolutionary genetics analysis version 7.0 for Bigger Datasets. *Molecular Biology and Evolution*, *33*(7), 1870–1874. https://doi.org/10.1093/molbev/msw054

Lambros, C., & Vanderberg, J. P. (1979). Synchronization of *Plasmodium falciparum* Erythrocytic Stages in Culture. *The Journal of Parasitology*, *65*(3), 418–420. https://doi.org/10.2307/3280287

Lanfrancotti, A., Bertuccini, L., Silvestrini, F., & Alano, P. (2007). *Plasmodium falciparum*: mRNA co-expression and protein co-localisation of two gene products upregulated in early gametocytes. *Experimental Parasitology*, *116*(4), 497–503. https://doi.org/10.1016/j.exppara.2007.01.021

Lévêque, M. F., Berry, L., Yamaryo-Botté, Y., Nguyen, H. M., Galera, M., Botté, C. Y., & Besteiro, S. (2017). TgPL2, a patatin-like phospholipase domain-containing protein, is involved in the maintenance of apicoplast lipids homeostasis in Toxoplasma. *Molecular Microbiology*, *105*, 158–174. https://doi.org/10.1111/mmi.13694

Livak, K. J., & Schmittgen, T. D. (2001). Analysis of Relative Gene Expression Data Using Real-Time Quantitative PCR and the $2-\Delta\Delta CT$ Method. *Methods*, *25*(4), 402–408. https://doi.org/10.1006/METH.2001.1262

Llinás, M. (2017). Less lipid, more commitment. *Cell*, *171*(7), 1474–1476. https://doi.org/10.1016/j.cell.2017.11.044

Malley, K. R., Koroleva, O., Miller, I., Sanishvili, R., Jenkins, C. M., Gross, R. W., & Korolev, S. (2018). The structure of iPLA2β reveals dimeric active sites and suggests mechanisms of regulation and localization. *Nature Communications*, *9*(1), 765. https://doi.org/10.1038/s41467-018-03193-0

Mi-Ichi, F., Kano, S., & Mitamura, T. (2007). Oleic acid is indispensable for intraerythrocytic proliferation of *Plasmodium falciparum*. *Parasitology*, *134*(12), 1671–1677. https://doi.org/10.1017/S0031182007003137

Mi-Ichi, F., Kita, K., & Mitamura, T. (2006). Intraerythrocytic *Plasmodium falciparum* utilize a broad range of serum-derived fatty acids with limited modification for their growth. *Parasitology*, *133*(4), 399–410. https://doi.org/10.1017/S0031182006000540

Mordue, D. G., Scott-Weathers, C. F., Tobin, C. M., & Knoll, L. J. (2007). A patatin-like protein protects *Toxoplasma gondii* from degradation in activated macrophages. *Molecular Microbiology*, *63*(2), 482–496. https://doi.org/10.1111/j.1365-2958.2006.05538.x

Ngwa, C. J., Kiesow, M. J., Papst, O., Orchard, L. M., Filarsky, M., Rosinski, A. N., … Pradel, G. (2017). Transcriptional profiling defines histone acetylation as a regulator of gene expression during human-to-mosquito transmission of the malaria parasite *Plasmodium falciparum*. *Frontiers in Cellular and Infection Microbiology*, *7*, 320. https://doi.org/10.3389/fcimb.2017.00320

Ngwa, C. J., Scheuermayer, M., Mair, G. R., Kern, S., Brügl, T., Wirth, C. C., … Pradel, G. (2013). Changes in the transcriptome of the malaria parasite *Plasmodium falciparum* during the initial phase of transmission from the human to the mosquito. *BMC Genomics*, *14*(1), 256. https://doi.org/10.1186/1471-2164-14-256

Pessi, G., Choi, J.-Y., Reynolds, J. M., Voelker, D. R., & Mamoun, C. B. (2005). In vivo evidence for the specificity of *Plasmodium falciparum* phos-pho-ethanolamine methyltransferase and its coupling to the Kennedy pathway. *The Journal of Biological Chemistry*, *280*(13), 12461–12466. https://doi.org/10.1074/jbc.M414626200

Pessi, G., Kociubinski, G., & Mamoun, C. B. (2004). A pathway for phosphatidylcholine biosynthesis in *Plasmodium falciparum* involving phos-pho-ethanolamine methylation. *Proceedings of the National Academy of Sciences of the United States of America*, *101*(16), 6206–6211. https://doi.org/10.1073/pnas.0307742101

Peterson, M. G., Marshall, V. M., Smythe, J. A., Crewther, P. E., Lew, A., Silva, A., … Kemp, D. J. (1989). Integral membrane protein located in the apical complex of *Plasmodium falciparum*. *Molecular and Cellular Biology*, *9*(7), 3151–3154.

Poran, A., Nötzel, C., Aly, O., Mencia-Trinchant, N., Harris, C. T., Guzman, M. L., … Kafsack, B. F. C. (2017). Single-cell RNA sequencing reveals a signature of sexual commitment in malaria parasites. *Nature*, *551*(7678), 95–99. https://doi.org/10.1038/nature24280

Pradel, G. (2007). Proteins of the malaria parasite sexual stages: Expression, function and potential for transmission blocking strategies. *Parasitology*, *134*(14), 1911–1929. https://doi.org/10.1017/S0031182007003381

Pradel, G., Hayton, K., Aravind, L., Iyer, L. M., Abrahamsen, M. S., Bonawitz, A., … Templeton, T. J. (2004). A multidomain adhesion protein family expressed in *plasmodium falciparum* is essential for transmission to the mosquito. *The Journal of Experimental Medicine*, *199*(11), 1533–1544. https://doi.org/10.1084/JEM.20031274

Prommana, P., Uthaipibull, C., Wongsombat, C., Kamchonwongpaisan, S., Yuthavong, Y., Knuepfer, E., … Shaw, P. J. (2013). Inducible knockdown of plasmodium gene expression using the glmS ribozyme. *PLoS ONE*, *8*(8), e73783. https://doi.org/10.1371/journal.pone.0073783

Przyborski, J. M., Miller, S. K., Pfahler, J. M., Henrich, P. P., Rohrbach, P., Crabb, B. S., & Lanzer, M. (2005). Trafficking of STEVOR to the Maurer's clefts in *Plasmodium falciparum*-infected erythrocytes. *The EMBO Journal*, *24*(13), 2306–2317. https://doi.org/10.1038/sj.emboj.7600720

Radfar, A., Méndez, D., Moneriz, C., Linares, M., Marín-García, P., Puyet, A., … Bautista, J. M. (2009). Synchronous culture of *Plasmodium falciparum* at high parasitemia levels. *Nature Protocols*, *4*(12), 1899–1915. https://doi.org/10.1038/nprot.2009.198

Ramakrishnan, S., Docampo, M. D., MacRae, J. I., Pujol, F. M., Brooks, C. F., van Dooren, G. G., … Striepen, B. (2012). Apicoplast and endoplasmic reticulum cooperate in fatty acid biosynthesis in apicomplexan parasite *Toxoplasma gondii*. *Journal of Biological Chemistry*, *287*(7), 4957–4971. https://doi.org/10.1074/jbc.M111.310144

Ramanadham, S., Ali, T., Ashley, J. W., Bone, R. N., Hancock, W. D., & Lei, X. (2015). Calcium-independent phospholipases A $_2$ and their roles in biological processes and diseases. *Journal of Lipid Research*, *56*(9), 1643–1668. https://doi.org/10.1194/jlr.R058701

Rea, E., Le Roch, K. G., & Tewari, R. (2018). Sex in *Plasmodium falciparum*: Silence Play between GDV1 and HP1. *Trends in Parasitology*, *34*(6), 450–452. https://doi.org/10.1016/j.pt.2018.04.006

Ryu, S. B. (2004). Phospholipid-derived signaling mediated by phospholipase A in plants. *Trends in Plant Science*, *9*(5), 229–235. https://doi.org/10.1016/J.TPLANTS.2004.03.004

Salanti, A., Staalsoe, T., Lavstsen, T., Jensen, A. T. R., Sowa, M. P. K., Arnot, D. E., … Theander, T. G. (2003). Selective upregulation of a single distinctly structured var gene in chondroitin sulphate A-adhering *Plasmodium falciparum* involved in pregnancy-associated malaria. *Molecular Microbiology*, *49*(1), 179–191. https://doi.org/10.1046/j.1365-2958.2003.03570.x

Schneweis, S., Maier, W. A., & Seitz, H. M. (1991). Haemolysis of infected erythrocytes ? a trigger for formation of *Plasmodium falciparum* gametocytes? *Parasitology Research*, *77*(5), 458–460. https://doi.org/10.1007/BF00931646

Senda, K., Yoshioka, H., Doke, N., & Kawakita, K. (1996). A Cytosolic Phospholipase A2 from Potato Tissues Appears to Be Patatin. *Plant and Cell Physiology*, *37*(3), 347–353. https://doi.org/10.1093/oxfordjournals.pcp.a028952

Shewry, P. R. (2003). Tuber storage proteins. *Annals of Botany*, *91*(7), 755–769. https://doi.org/10.1093/aob/mcg084

Shohdy, N., Efe, J. A., Emr, S. D., & Shuman, H. A. (2005). Pathogen effector protein screening in yeast identifies Legionella factors that interfere with membrane trafficking. *Proceedings of the National Academy of Sciences of the United States of America*, *102*(13), 4866–4871. https://doi.org/10.1073/pnas.0501315102

Simões, A. P., Roelofsen, B., & Op den Kamp, J. A. (1992). Incorporation of free fatty acids can explain alterations in the molecular species composition of phosphatidylcholine and phosphatidylethanolamine in human erythrocytes as induced by *Plasmodium falciparum*. *Cell Biology International Reports*, *16*(6), 533–545. https://doi.org/10.1016/S0309-1651(05)80052-9

Simon, N., Scholz, S. M., Moreira, C. K., Templeton, T. J., Kuehn, A., Dude, M.-A., & Pradel, G. (2009). Sexual stage adhesion proteins form multi-protein complexes in the malaria parasite *Plasmodium falciparum*. *The Journal of Biological Chemistry*, *284*(21), 14537–14546. https://doi.org/10.1074/jbc.M808472200

Singh, P., Alaganan, A., More, K. R., Lorthiois, A., Thiberge, S., Gorgette, O., … Chitnis, C. E. (2019). Role of a patatin-like phospholipase in *Plasmodium falciparum* gametogenesis and malaria transmission. *Proceedings of the National Academy of Sciences of the United States of America*, *116*(35), 17498–17508. https://doi.org/10.1073/pnas.1900266116

Sinha, A., Hughes, K. R., Modrzynska, K. K., Otto, T. D., Pfander, C., Dickens, N. J., … Waters, A. P. (2014). A cascade of DNA-binding proteins for sexual commitment and development in Plasmodium. *Nature*, *507*(7491), 253–257. https://doi.org/10.1038/nature12970

Spork, S., Hiss, J. A., Mandel, K., Sommer, M., Kooij, T. W. A., Chu, T., … Przyborski, J. M. (2009). An unusual ERAD-like complex is targeted to the apicoplast of *Plasmodium falciparum*. *Eukaryotic Cell*, *8*(8), 1134–1145. https://doi.org/10.1128/EC.00083-09

Tischer, M., Pradel, G., Ohlsen, K., & Holzgrabe, U. (2012). Quaternary ammonium salts and their antimicrobial potential: Targets or nonspecific interactions? *ChemMedChem*, *7*(1), 22–31. https://doi.org/10.1002/cmdc.201100404

Tobin, C. M., & Knoll, L. J. (2012). A patatin-like protein protects Toxoplasma gondii from degradation in a nitric oxide-dependent manner. *Infection and Immunity*, *80*(1), 55–61. https://doi.org/10.1128/IAI.05543-11

Trager, W., & Jensen, J. B. (1976). Human malaria parasites in continuous culture. *Science (New York, N.Y.)*, *193*(4254), 673–676. https://doi.org/10.1126/science.781840

Tran, P. N., Brown, S. H. J., Rug, M., Ridgway, M. C., Mitchell, T. W., & Maier, A. G. (2016). Changes in lipid composition during sexual development of the malaria parasite *Plasmodium falciparum*. *Malaria Journal*, *15*(1), 73. https://doi.org/10.1186/s12936-016-1130-z

Usui, M., Prajapati, S. K., Ayanful-Torgby, R., Acquah, F. K., Cudjoe, E., Kakaney, C., … Williamson, K. C. (2019). Publisher Correction: *Plasmodium falciparum* sexual differentiation in malaria patients is associated with host factors and GDV1-dependent genes. *Nature Communications*, *10*(1), 2740. https://doi.org/10.1038/s41467-019-10805-w

Vial, H. J., Eldin, P., Tielens, A. G. M., & Van Hellemond, J. J. (2003). Phospholipids in parasitic protozoa. *Molecular and Biochemical Parasitology*, *126*(2), 143–154. https://doi.org/10.1016/S0166-6851(02)00281-5

Vial, H. J., & Ben Mamoun, C. (2005). Plasmodium lipids: Metabolism and function. In I. W. Sherman (Ed.), *Molecular Approaches to Malaria* (pp. 327–352). Washington, DC: American Society of Microbiology. https://doi.org/10.1128/9781555817558.ch17

Wang, Y., Geer, L. Y., Chappey, C., Kans, J. A., & Bryant, S. H. (2000). Cn3D: Sequence and structure views for Entrez. *Trends in Biochemical Sciences*, *25*(6), 300–302. https://doi.org/10.1016/S0968-0004(00)01561-9

Wein, S., Ghezal, S., Buré, C., Maynadier, M., Périgaud, C., Vial, H. J., … Cerdan, R. (2018). Contribution of the precursors and interplay of the pathways in the phospholipid metabolism of the malaria parasite. *Journal of Lipid Research*, *59*(8), 1461–1471. https://doi.org/10.1194/jlr.M085589

Weißbach, T., Golzmann, A., Bennink, S., Pradel, G., & Julius Ngwa, C. (2017). Transcript and protein expression analysis of proteases in the blood stages of *Plasmodium falciparum*. *Experimental Parasitology*, *180*, 33–44. https://doi.org/10.1016/j.exppara.2017.03.006

Wilson, S. K., & Knoll, L. J. (2018). Patatin-like phospholipases in microbial infections with emerging roles in fatty acid metabolism and immune regulation by Apicomplexa. *Molecular Microbiology*, *107*(1), 34–46. https://doi.org/10.1111/mmi.13871

Wirth, C. C., Bennink, S., Scheuermayer, M., Fischer, R., & Pradel, G. (2015). Perforin-like protein PPLP4 is crucial for mosquito midgut infection by *Plasmodium falciparum*. Molecular and Biochemical Parasitology, 201(2), 90–99. https://doi.org/10.1016/j.molbiopara.2015.06.005

Wirth, C. C., Glushakova, S., Scheuermayer, M., Repnik, U., Garg, S., Schaack, D., … Pradel, G. (2014). Perforin-like protein PPLP2 permeabilizes the red blood cell membrane during egress of *Plasmodium falciparum* gametocytes. *Cellular Microbiology*, *16*(5), 709–733. https://doi.org/10.1111/cmi.12288

World Health Organisation (2018). *World Malaria Report 2018*. Geneva: WHO. https://doi.org/10.4135/9781452276151.n221

Yang, J., Yan, R., Roy, A., Xu, D., Poisson, J., & Zhang, Y. (2015). The I-TASSER Suite: Protein structure and function prediction. *Nature Methods*, *12*(1), 7–8. https://doi.org/10.1038/nmeth.3213

Zhu, W., Hammad, L. A., Hsu, F., Mao, Y., & Luo, Z.-Q. (2013). Induction of caspase 3 activation by multiple Legionella pneumophila Dot/Icm substrates. *Cellular Microbiology*, *15*(11), 1783–1795. https://doi.org/10.1111/cmi.12157

SUPPORTING INFORMATION

Additional supporting information may be found online in the Supporting Information section at the end of this article.

How to cite this article: Flammersfeld A, Panyot A, Yamaryo-Botté Y, et al. A patatin-like phospholipase functions during gametocyte induction in the malaria parasite *Plasmodium falciparum*. *Cellular Microbiology*. 2020;22:e13146. https://doi.org/10.1111/cmi.13146